Responses to the comments of the Editor (E. Boss)

We thank you very much for your attentive reading and for the suggestions you proposed on the manuscript BG-2015-25. In most cases, we changed the text accordingly to your suggestions (see the track-changes version below). In the following, we provide a specific response to some of your comments.

Page 7, line 13:

Text:

"Profiles with a surface fluorescence value lower than the bottom value were removed from the database (202 profiles removed)."

Editor comment:

"this can be real (that is not instrumental failure) and may be due to dissolved substances at depth, e.g. Rottgers and Kock, 2012, BG"

Authors response:

Most of the profiles with a surface fluorescence value lower than the bottom value display also a relatively shallow depth for their deepest observation. Indeed, for 90% of these profiles, their deepest observation depth was above 177m. Yet, at this depth, in oligotrophic conditions, the presence of fluorescence can be due to chlorophyll. Then, we considered that these profiles are likely incomplete on the vertical and we preferred to remove them from the dataset.

Page 9, line 16:

Text:

"considering that the median of the ten deepest observations is equal to zero "

Editor comment:

"Due to the problem with CDOM we find that the zero is not necesserily at the deepest depth, but rather there can be at mid profile. This is probably a better value to adjust agains (e.g. 10 minimal values in a profile)"

Authors response:

Although profiles have been filtered, some noise remains. Hence, using the ten minimal values to compute beta should result in an underestimation of beta. Even if we agree that CDOM could affect the chlorophyll fluorescence profile, a visual control of the whole database did not drive to the detection of artefacts like increases of fluorescence at depth. Then, to compute beta, we preferred to maintain our method, based on the ten deepest observations.

Page 10, line 14:

Editor comment:

1 "Make sure to provide the Ze calculation method in the methods section."

2 Authors response:

3 In section method we added the following sentence to explain the Ze calculation method:

4 "Z_e is calculated from the chlorophyll integrated content using equations of Morel and
5 Berthon (1989)"

6 **Page 14 line 19:**

7 Text:

8 "According to Huisman et al., (1999), the development of a [Chl-a] gradient in the mixed
9 layer would be possible if mixed layer turbulence were low thus allowing for the
10 accumulation of phytoplankton cells near the surface. "

11 Editor comment:

12 "you can test for that with a less stringent MLD criterion, e.g. 0.005kg/m^3"

13 Author response:

14 You are right. When the MLD is computed with a difference density criteria of 0.05 kg m^{-3},
15 MLD ranges between 11 and 49m which supports the hypothesis of Huisman et al. (1999).

16

17 **Page 14 line 21:**

18 Text:

19 "Lowest surface [Chl-a] values are observed for "DCM" shape profiles while highest (1.22
20 mg m-3) values are observed for "HSC" shape profiles."

21 Editor comment:

22 "these are also the ones for which you cannot fully correct for NPQ"

23 Authors response:

24 Surface chlorophyll values reported on Table 3 derived from ocean color observations (see
25 figure caption). Then, they are not affected by NPQ. In the new version of the manuscript, we
26 added a mention about the remote sensing origin of surface chlorophyll data:

27 Page 14, line 22: "According to the results presented in Table 3, ocean color surface [Chl-a]
28 values are related to the shape of the vertical profile."

29

30 **Page 17 line 4:**

31 Text:

32 "We hypothesize that these winter subsurface maxima could be an artifact caused by the large
33 averaging timescale (from December to March), leading to the combination of [Chl-a] profiles
34 with highly different vertical distributions (see Fig. 5) "

35 Editor comment:

36 "Can you test this?"

37 Authors response:

38 The comparison of the monthly (Fig. 3) and seasonal (Fig. 5) fluorescence-based chlorophyll
39 climatology is a sort of test for this hypothesis.

1

Page 19 line 31:

Text:

"The observation of "HSC" like profiles in the South-West region suggests that, during winter, mixing is able to supply enough nutrients at the surface to support episodic developments of phytoplankton close to the surface, when water column begins to stabilize."

Editor comment:

"Are the physical forcings different between East and West? e.g. 1D and weak horizontal density gradients in the East and more eddies/3D instabilities/strong horizontal density gradients in the West in Winter? More homogeneous forcing in the East vs. strong frontal features in the West? That could also contribute to the observations."

Authors response:

It is very hard to determine which could explain the observed biological differences between south-west and east Mediterranean Sea. In both regions, sub-mesoscale activity is very important with fronts, jets and eddies. Eddy Kinetic Energy has similar intensity in east and west Mediterranean Sea (see Rio et al., 2007, Journal of Marine Systems). To our mind, as exposed in the text, differences in chlorophyll patterns would be due to the nutrient distribution and concentration which are affected by the eastward circulation of the surface Modified Atlantic Waters.

However, we mentioned your hypothesis in the new version of the manuscript:

Page 20, line 7: "As sub-mesoscale activity, associated to jets, fronts and eddies, is similarly intense in both, South-Western and Eastern basins (Rio et al., 2007), our best explanation for the spatial divergences in the occurrence of "HSC" profiles is the regional differences in nutrient stocks below the nitracline."

Page 22 line 10

Text:

"However, according to Table 4, the estimations of nitracline depths are not likely to be good estimators of the top of the nitracline, if the nitrate gradient is not a enough sharp feature, as is it the case, for example in the Eastern Mediterranean Sea. Indeed, nitracline depths have been computed from discrete vertical 10 profiles, using the 1µM isoline (Lavigne et al., 2013)."

Editor comment:

"that is probably due to the poor vertical resolution of data collected with bottles. Should be much better with sensors measuring at higher vertical resolution."

Authors response:

You are right, we also mentioned it in the text (page 22, line 10-11), poor vertical resolution does not allow to properly estimate the nitracline depth. However, we think that this problem is worse when the vertical nitrate distribution does not display a sharp and clear gradient between surface and deep waters as it is the case in the Eastern Mediterranean Sea (see for instance http://www.oao.obs-vlfr.fr/bioargo/PHP/lovbio018c/lovbio018c.html).

Tables

3

1   As recommended, in tables 2 and 3, non-parametric metrics have been used.

2

On the vertical distribution of the chlorophyll-a concentration in the Mediterranean Sea: a basin scale and seasonal approach

H. Lavigne[1], F. D'Ortenzio[2,3], M. Ribera D'Alcalà[4], H. Claustre[2,3], R. Sauzède[2,3] and M. Gacic[1]

[1]{Istituto Nazionale di Oceanografia e di Geofisica Sperimentale – OGS, Dip. di Oceanografia, Borgo Grotta Gigante 42/c, 34010 Sgonico (Trieste), Italy}

[2]{CNRS, UMR 7093, Laboratoire d'Océanographie de Villefranche, 06230 Villefranche sur-Mer, France}

[3]{Université Pierre et Marie Curie-Paris 6, UMR 7093, Laboratoire d'Océanographie de Villefranche, 06230 Villefranche-sur-Mer, France}

[4]{Laboratorio di Oceanografia Biologica, Stazione Zoologica "A. Dohrn", Villa Comunale, Napoli, Italy}

Correspondence to: H. Lavigne (hlavigne@ogs.trieste.it)

1   **Abstract**

2   The distribution of the chlorophyll-a concentration ([Chl-a]) in the Mediterranean Sea, mainly

3   obtained from satellite surface observations or from scattered in situ experiments, is updated

4   by analyzing a database of fluorescence profiles converted into [Chl-a]. The database, which

5   includes 6790 fluorescence profiles from various origins, was processed with a specific

6   quality control procedure. To ensure homogeneity between the different data sources, 65% of

7   fluorescence profiles have been inter-calibrated on the basis of their concomitant satellite

8   [Chl-a] estimation. The climatological pattern of [Chl-a] vertical profiles in four key sites of

9   the Mediterranean Sea has been analyzed. Climatological results confirm previous findings

10   over the range of existing [Chl-a] values and throughout the principal Mediterranean trophic

11   regimes. It also provides new insights on the seasonal variability of the shape of the vertical

12   [Chl-a] profile, inaccessible from remote sensing observations. An analysis based on the

13   recognition of the general shape of the fluorescence profile was also performed. Although the

14   shape of [Chl-a] vertical distribution characterized by a deep chlorophyll maximum (DCM) is

15   ubiquitous during summer, different forms are observed during winter, thus suggesting that

16   factors affecting the vertical distribution of the biomass are complex and highly variable. The

17   [Chl-a] spatial distribution in the Mediterranean Sea mimics, at smaller scales, what is

18   observed in the Global Ocean. As already evidenced by analyzing satellite surface

19   observations, mid-latitude and subtropical like phytoplankton dynamics coexist in the

20   Mediterranean Sea. Moreover, the Mediterranean DCM variability appears to be characterized

21   by patterns already observed at the Global scale.

22

1   Introduction

1.1 Surface chlorophyll distribution

Chlorophyll-a concentration ([Chl-a] hereafter) is the main proxy of phytoplankton biomass (Strickland, 1965; Cullen, 1982), representing a key oceanic biogeochemical variable. However, in the Mediterranean Sea, as in the global ocean, the comprehensive knowledge of the [Chl-a] spatio-temporal variability has been prevented due to a lack in in situ observations (Conkright et al., 2002; Manca et al., 2004). The understanding of the [Chl-a] distribution is essentially restricted to the surface, as based on remote sensing observations. In the Mediterranean Sea, ocean color sensors, like CZCS (Feldman et al., 1989) or SeaWiFS (McClain et al., 1998), provide observations with high temporal and spatial resolution over the whole basin (Morel and André, 1991; Antoine et al., 1995; Bosc et al. 2004).

As in situ observations have demonstrated (Dolan et al., 1999; Dolan et al., 2002; Ignatiades et al., 2009), satellite data confirm the oligotrophic nature of the basin (Dugdale and Wilkerson, 1988) as well as the east-west gradient in oligotrophy (see Fig. 1, panels B and C). Excepting the Liguro-Provençal region, where a large spring bloom takes place, and for some localized spots, most of the basin exhibits very low values (< 0.2 mg m^{-2}) of satellite surface [Chl-a]. Surface [Chl-a] decreases eastward (Bosc et al., 2004; Barale et al., 2008) displaying a sharp gradient between the west and east basins (mean [Chl-a] is about 0.4 mg m^{-3} in the west basin and 0.05 mg m^{-3} in the east basin, Bosc et al., 2004, Fig. 1, panels B and C). Superimposed on this general pattern, ocean color data also provide insights on the occurrence and on the influence of meso and sub-mesoscale structures on [Chl-a] (Taupier-Letage et al., 2003; Navarro et al., 2011, D'Ortenzio et al., 2014).

Satellite observations have also been the primary source of information for the characterization of the [Chl-a] seasonal and interannual variability (D'Ortenzio and Ribera d'Alcalà, 2009; Volpe et al., 2012; Lavigne et al., 2013). At a Global scale, ocean color satellite observations indicate that surface [Chl-a] annual cycles display different patterns moving from a tropical to a temperate or a polar environment (Yoder et al., 1993) generally following latitudinal gradients. Boundaries between large ecological regions have been determined from satellite observations, in the global ocean (Longhurst, 2006) but also at regional scales (Devred et al., 2007; D'Ortenzio and Ribera d'Alcalà, 2009; Platt et al., 2010). Indeed, focusing on ocean color observations, D'Ortenzio and Ribera d'Alcalà (2009) confirmed the presence, in the Mediterranean Sea, of surface [Chl-a] annual cycles, displaying

3

1 similarities with subtropical or with temperate regions. The authors demonstrated that a
2 subtropical-like [Chl-a] seasonality (highest [Chl-a] during winter and lowest during summer)
3 encompasses most of the basin whereas a temperate like seasonality, marked by a high peak
4 of surface [Chl-a] in spring (in March/April), is recurrently observed in the North-Western
5 basin and occasionally in other Mediterranean regions. Further analysis (Lavigne et al., 2013)
6 showed that the coexistence of different regimes in the Mediterranean Sea is mainly due to the
7 high variability of the interplay between physical forcing, which affects the Mixed Layer
8 Depth (MLD hereafter), and chemical forcing (i.e. nutrient availability).

9 **1.2 The vertical [Chl-a] distribution**

10 Contrary to the horizontal distribution of [Chl-a] which, despite the uncertainties due to the
11 impact of bio-optical processes (see below), are regularly assessed within the basin, low cloud
12 coverage allowing for high frequency measurements, vertical distributions of [Chl-a] are
13 much less documented due to in situ undersampling and to the intrinsic limits of color remote
14 sensing in the retrieval of information from subsurface layers.

15 So far, the largest part of the information derives from studies conducted in specific sites (e.g.,
16 Dolan et al., 2002; Christaki et al., 2001; Estrada et al., 1993; Casotti et al., 2003; Marty et al.,
17 2002; Psarra et al., 2000; Krom et al., 1992), generalizations based on large scale cruises
18 (Moutin and Raimbault, 2002; Crombet et al, 2011) and synthetic analyses (e.g. Siokou-
19 Frangou et al., 2012), or reconstructions derived from modeling studies (e.g., Macias et al.,
20 2014; Crise et al., 1999). These studies showed that deep chlorophyll maximum (DCM,
21 hereafter) are ubiquitous over the Mediterranean from spring to autumn (Crise et al., 1999;
22 Moutin and Raimbault 2002; Siokou-Frangou et al., 2010). They display a longitudinal
23 deepening from West to East (see Crise et al., 1999 for a review), with their depth ranging
24 from 30 m in the westernmost area (Dolan et al., 2002) to 70 m in the South Adriatic and even
25 more than 100 m in the Levantine Sea (Christaki et al., 2001). During winter, DCM generally
26 disappear in the whole basin and the so called "mixed" shape (Morel and Berthon, 1989; Uitz
27 et al., 2006), characterized by a constant [Chl-a] from the surface to the basis of the MLD is
28 often observed (Krom et al., 1992; Marty et al., 2002; Mignot et al., 2014). Alternatively, a
29 [Chl-a] vertical shape marked by a high subsurface maximum close to the surface (less than
30 10m) has also been documented for the North-Western basin, during the spring bloom period
31 (Marty et al., 2002; Manca et al., 2004). In spite of those focused studies and the compilation
32 of Chl-a climatology provided by the MEDAR/MEDATLAS project (Maillard and Coauthors,

2005), the spatial distribution of [Chl-a] vertical profiles and their yearly patterns are still poorly documented in the basin. Satellite [Chl-a] values may provide additional information using the approach introduced for global assessments of depth integrated Chl-a values (e.g., Morel and Berthon, 1989). In many instances, (e.g., Bosc et al., 2004) their use was implicit and no specific analysis on the vertical distribution *per se* was carried out.

As discussed in a recent review by Cullen (2015), there is no unique DCM and its dynamics result from the interactions among external forcing, e.g., the penetration of light in water, the intensity of vertical mixing and subsurface nutrient distribution and biotic processes, e.g., photoacclimation, grazing, phytoplankton composition. To assess which and how many DCMs exist in the Mediterranean sea because of its known geographical and dynamical gradients, a starting step is to produce a quantitative characterization of their shapes and their seasonal evolution, which is one of the main scope of this contribution. In addition, a good appreciation of seasonal changes in vertical [Chl-a] distribution, the other objective of this study, is a first step towards a better understanding of mechanisms controlling seasonal phytoplankton development. It is also essential to better interpret changes in surface [Chl-a] as detected by satellite sensors. This study will ~~allow~~help for the ~~integration of the~~ biogeographical ~~characterization of the basin built on~~ interpretation of surface [Chl-a] patterns, ~~thus~~ paving the way to focused area studies based on in situ sampling or autonomous vehicles.

1.3 Fluorescence

In situ [Chl-a] are obtained on filtered water samples, from which the pigment content was extracted and analyzed. The most accurate results are nowadays obtained by High Performance Liquid Chromatography (HPLC, Gieskes and Kraay, 1983). Their associated protocols are most often expensive, time consuming, and depend on direct sampling with bottles. They hence provide discrete values on a vertical scale with a limited horizontal and temporal resolution. To overcome the above limitations, fluorescence observations can be used. The estimation of [Chl-a] from the fluorescence technique (Lorenzen, 1966) is based on the chlorophyll-a property of absorbing blue light and re-emitting it, as fluorescence, in the red part of the spectrum. The quantity of fluorescence emitted by a water sample is proportional to [Chl-a], which could be then easily derived by measuring emitted radiation at red wavelengths. The fluorescence technique therefore represents a ~~robust and~~ non-invasive method to observe continuous vertical profiles of [Chl-a]. Nowadays, fluorimeters commonly

equip CTDs and can even be built in autonomous profilers. Indeed, an increasing number of profiling floats and gliders are equipped with a fluorimeter (Johnson et al., 2009) while fluorescence is becoming the main source of data for [Chl-a] vertical profiles. To date, more than 67900 fluorescence profiles are available in the World Ocean Database 2013 (Boyer et al., 2013).

However, fluorescence is only a proxy for [Chl-a], implying that the fluorescence signal need to be calibrated for a [Chl-a] estimation. Calibration coefficients (α and β, see Eq. (1)) provided by manufacturers are only indicative of the response of the sensor to a given Chl-a concentration in an extract or in an algal suspension, and cannot be applied to all in situ conditions. The fluorescence to [Chl-a] ratio is highly variable, since it changes with the taxonomic assemblage or environmental conditions (Kiefer, 1973). or it may be affected by dissolved materials (Rottgers and Koch, 2012). For instance, under low light conditions, the chlorophyll content per cell can increase while the fluorescence to [Chl-a] ratio decreases due to the packaging effect (Sosik et al., 1989). In response to supra-optimal light irradiation, phytoplankton triggers photo-protection mechanisms, inducing a drastic decrease in the fluorescence to [Chl-a] ratio (Kolber and Falkowski, 1993; Müller et al., 2001); this mechanism is called Non Photochemical Quenching (NPQ). The main result of NPQ effect is a decrease of fluorescence at the surface, even for constant [Chl-a] (Cullen and Lewis, 1995; Xing et al., 2012).

$$[Chl - a] = \alpha \times (FLUO - \beta) \quad Eq.(1)$$

Better estimates are obtained by determining the empirical coefficients (i.e. α and β) that fit fluorescence with in situ data for each profile (Morel and Maritorena, 2001) or for each cruise (Sharples et al., 2001; Strass, 1990; Cetinic et al., 2009). However, this calibration method based on the existence of simultaneous in situ samples is not always applicable. Alternative calibration methods, independent of concomitant HPLC observations, have therefore recently been developed (Boss et al., 2008; Xing et al., 2011; Mignot et al., 2011; Lavigne et al., 2012). They are based on additional information such as irradiance profiles (Xing et al., 2011), ocean color observations (Boss et al., 2008; Lavigne et al., 2012) or the shape of the fluorescence profile (Mignot et al., 2011). Although these new calibration methods do not reach the accuracy of HPLC based calibration, they offer an acceptable alternative to extract reliable estimates of [Chl-a] vertical profiles from large quantity of fluorescence profiles.

1.4 Outlines

1   This study aims at improving knowledge on the spatio-temporal variability of the vertical

2   distribution of the [Chl-a] in the Mediterranean Sea, focusing particularly on [Chl-a]

3   seasonality. For this, all the available proxies of [Chl-a] ~~were~~are merged to build a new data

4   base. Special attention ~~was~~is paid to the shape of the [Chl-a] profiles: indeed different patterns

5   can point to different processes controlling the phytoplankton distribution. The spatial and

6   seasonal variability of the DCM, which is one of the most common features in Mediterranean

7   [Chl-a] vertical profiles, ~~will be~~is also specifically investigated. The scope of this paper is

8   ~~essentially restrained to~~ the description of the variability of [Chl-a] vertical profiles, as they

9   result from the interactions between many factors that can be complex as well as poorly

10 documented. This variability ~~will be~~is only discussed with regard to Mediterranean hydrology

11 and light fields.

12 In the following section, the fluorescence database is presented, including the quality control

13 and calibration procedures that were applied. In the results section, the seasonal and spatial

14 variability of climatological [Chl-a] vertical profiles, derived from fluorescence-based

15 reconstructed [Chl-a] profiles is presented. Climatological results are completed by the

16 analysis of the shape of the [Chl-a] profiles. Contrary to the climatology of [Chl-a] vertical

17 profiles, the shape analysis is based on normalized [Chl-a] profiles and does not account for

18 the [Chl-a] values. The seasonal variability in occurrences of principal [Chl-a] vertical shapes

19 is also investigated here. In the fourth section, certain methodological points related to the

20 production of climatological patterns are addressed. Results ~~presented in above mentioned~~

21 ~~section~~ are also compared with previous remote sensing based observations. Finally, the

22 diversity in Mediterranean [Chl-a] patterns is highlighted in a comparison with the Global

23 Ocean.

24 **2   Data and Methods**

25 **2.1 Data set of fluorescence chlorophyll profiles**

26 More than 6000 chlorophyll fluorescence profiles, and their corresponding temperature and

27 salinity profiles, from the Mediterranean Sea in areas where bathymetry exceeds 100m depth,

28 were collected from various data source (Table 1). These comprise online databases (986

29 profiles), French cruises (2670 profiles), the MEDAR (228 profiles) and the SESAME

30 programs data base (1815 profiles) and, finally, fluorescence profiles derived from Bio-Argo

31 floats (1091 profiles). The density of profiles covers the whole Mediterranean Basin, although

1 some areas are better represented than others (Fig. 1). Many profiles are available in the

2 North-Western Mediterranean Sea, whereas the South-Western Mediterranean Sea and the

3 Levantine Sea are poorly represented. Available profiles range between 1994 and 2014, all

4 seasons being equally represented (winter 30% of data, spring 21%, summer 25% and autumn

5 24%). Although only 16% of the database are Bio-Argo profiles, they represent half of

6 available profiles for the 2008-2014 period.

7 **2.2 Data processing and calibration**

8 Prior to calibration, a quality control procedure was applied to fluorescence profiles. It

9 comprises a test of uniqueness (to eliminate repetitions of a same profile), the identification of

10 spikes (see D'Ortenzio et al., 2010) and of the signs of fluorometer failure (portion of profile

11 with exactly the same value or jumps in the fluorescence profile). After this quality control

12 step, 593 profiles were removed from the database. Then, incomplete profiles (i.e. profiles for

13 which the acquisition was not deep enough to display the whole fluorescence shape) were also

14 removed. Profiles with a surface fluorescence value lower than the bottom value were

15 removed from the database (202 profiles removed). In addition, the profiles obtained during

16 the three "Long Duration" stations of the BOUM cruise (Moutin et al., 2012) were removed

17 from the dataset, because they had been sampled at very high temporal frequency within

18 anticyclonic eddy (Moutin and Prieur, 2012). These 404 profiles, which are therefore not

19 independent, would have over-represented specific environments in the dataset.

20 The remaining fluorescence profiles (5571 profiles) were calibrated using satellite ocean color

21 matchups as surface references (Lavigne et al., 2012). This method has been validated in the

22 Mediterranean Sea, by comparing satellite calibrated profiles and in situ HPLC [Chl-a] data.

23 In the Mediterranean Sea, the calibrated profiles are unbiased and present a median error of

24 41%, which is reduced to 34% when compared to climatological averages. In summary, (see

25 Lavigne et al., 2012, for a comprehensive description and validation of the procedure) the

26 method consists in (step 1) a correction for the NPQ effect, (step 2) the adjustment to a zero

27 value of the fluorescence profile at depth and (step 3) the application of a calibration

28 coefficient obtained from ocean color satellite matchups. The last step has only been applied

29 to the fluorescence profiles available for the 1998-2014 period (i.e. time during which the

30 SeaWiFS or MODIS Aqua data were available and could be used to calculate the matchups).

31 Step 1 provides a systematic correction of the NPQ effect by extrapolating the maximum

32 fluorescence value observed in the mixed layer up to the surface (Xing et al. 2012). Although

1　Biermann et al. (2014) proposed an improvement of the method for profiles with euphotic

2　depth above MLD, we preferred to use a unique data processing procedure, to avoid the

3　introduction of an artificial bias due to a heterogenic data treatment. The MLD was evaluated

4　from potential density profiles using a density criterion of 0.03 kg m^{-3} (de Boyer Montegut et

5　al., 2004; D'Ortenzio et al., 2005). This method revealed to be an efficient NPQ correction in

6　most of conditions (Xing et al., 2012; Lavigne et al., 2012), although it presented limitations

7　for shallow MLD and stratified water columns. By applying the equation proposed by

8　Sackmann et al. (2008) on monthly averaged light fields, the impact of NPQ was observed to

9　be significant only above 60m, thus leading a two-fold underestimation of surface [Chl-a].

10　Considering this result, the weak efficiency of the NPQ correction method in stratified

11　conditions should not have major consequences on the present study. Only the analysis of the

12　surface to integrated content chlorophyll ratio (see Table 3) should be considered with

13　caution.

14　Step 2 corrects the systematic instrumental offset, which impacts on the whole profile,

15　although it can only be detected at depth. Except for very specific cases, [Chl-a] is considered

16　reach a zero value at depths where there is no more light availability. If it is not the case, a

17　correction factor (i.e. β on Eq. (1)) is subtracted from the whole fluorescence profile,

18　considering that the median of the ten deepest observations is equal to zero. Profiles in which

19　MLD was deeper than the deepest fluorescence observation were not processed but not

20　~~remove~~removed of the database (1.1% of data set). After step 1 and step 2 procedures, 5571

21　profiles were successfully corrected and stored in the so-called "1994-2014 database". These

22　fluorescence profiles were used later for the shape analysis (see Sect. 2.3 and Sect. 3.2).

23　In step 3, fluorescence profiles collected after 1998 were converted into [Chl-a] units using a

24　transformation based on ocean color satellite observations (Lavigne et al., 2012). 8-day Level

25　3 standard mapped images of SeaWiFS and MODIS Aqua surface chlorophyll at 9km

26　resolution were obtained from the NASA web site (http://oceancolor.gsfc.nasa.gov/) for the

27　1998-2014 period (1998-2007 for SeaWiFS and 2008-2014 for MODIS Aqua). The use of

28　NASA [Chl-a] standard products allows for a good consistency between SeaWiFS and

29　MODIS datasets thus avoiding the introduction of any bias between the two time-series

30　(Franz et al., 2005). For each fluorescence profile, the satellite image matching the profile

31　date was selected. The corresponding surface [Chl-a] values over a 0.1° x 0.1° box centered

32　on the geographical position of the profile were extracted and averaged. The integrated

33　chlorophyll content over $1.5Z_e$ (where Z_e is the euphotic depth) is then estimated from

satellite [Chl-a] using empirical relationships (Uitz et al., 2006~~).~~) and Z_e is calculated from the chlorophyll integrated content using equations of Morel and Berthon (1989). A multiplicative coefficient (α coefficient in Eq. (1)) is applied to the fluorescence profile, imposing that the integrated fluorescence content matches the integrated chlorophyll content derived from satellite. At the end, 3867 fluorescence profiles were successfully transformed into [Chl-a]. These [Chl-a] profiles formed the "1998-2014 database" and similarly to fluorescence profiles of the "1994-2014 database", they are available upon request from the first author.

2.3 Determination of the shape of fluorescence profiles

On the basis of a visual analysis of the whole database, five general types of fluorescence vertical shapes were identified. These five categories, which represent the most frequent shapes of vertical distribution observed in the Mediterranean, also reflect their conditioning by physical-biological processes. These categories are referred to as "DCM", "homogeneous", "HSC" (for High Surface Chlorophyll), "complex" and "modified DCM" on the basis of their general characteristics (Fig. 2). The "DCM" and "homogeneous" shapes have been commonly used to describe [Chl-a] vertical profiles (Morel and Berthon, 1989; Uitz et al., 2006; Mignot et al., 2011). They are referred to as "stratified" and "mixed", respectively, and are discriminated according to the relative position of Ze and MLD. The "DCM" shape is characterized by a subsurface DCM, and the "homogeneous" shape by a positive homogeneous [Chl-a] in the mixed layer. After examination of the database, three other standard shapes have been introduced (i.e. "HSC", "modified DCM" and "complex" shapes) to better describe the observed variability. The "HSC" standard shape was defined for profiles displaying a steady decrease of [Chl-a] from surface to depth (~100m) as generally observed during phytoplankton blooms (Chiswell, 2011). The "modified DCM" shape describes profiles with relatively high values in the mixed layer and with a peak of [Chl-a] just below the MLD. It represents an intermediate condition between the "DCM" and "homogeneous" situations. Finally, profiles with a complex shape, often displaying several peaks and a relatively high surface [Chl-a] were classed as standard "complex" shapes.

To automatically categorize each profile of the 1994-2014 database into one of the five shape classes, a simple algorithm has been used, computing the following metrics for each profile: the depth of fluorescence maxima (D_{max}, see Fig. 2 panels A and D), the MLD, the fluorescence integrated content in a 20m layer centered on D_{max} (F_{max}, see Fig. 2, panel A), the fluorescence integrated content in the 0-20m surface layer (F_{surf}, see Fig. 2 panel A), the

1 fluorescence integrated content in the mixed layer (F_{MLD}, see Fig. 2 panel D) and the total

2 fluorescence content (F_T, see Fig. 2 panel B).

3 The algorithm was applied to each profile. It first tests the "HSC" shape. The "HSC" shape is

4 assigned to a profile, if its fluorescence averaged over layers of 10m width decreases from

5 surface to 100m. Secondly, the "DCM" shape is tested. If MLD is above D_{max} and if F_{max} is

6 twice superior to F_{surf}, the profile is classed in the "DCM" category. If not, the

7 "homogeneous" shape is tested. The profile is classed in the "homogeneous" category if

8 F_{MLD}/F_T is superior to 0.85 (more than 85% of biomass contained in the mixed layer). Finally,

9 if the fluorescence profile does not meet any of the previous criteria, it is either classed in the

10 "modified DCM" category, if the corresponding MLD is above D_{max} or in the "complex"

11 category.

12 Overall, 2780 profiles were classed in the "DCM" category, 751 in the "homogeneous"

13 category, 413 in the "HSC" category, 637 in the "modified DCM" category and 990 in the

14 "complex" category.

15 **3   Results**

16 **3.1 Some climatological behaviors**

17 Although the availability of the calibrated profiles (1998-2014 database) should allow to

18 generate interpolated products on a regular mesh grid (as, for example, the World Ocean

19 Atlas, Conkright et al., 2002), we preferred to avoid any large interpolation and only present

20 Mediterranean patterns for locations well represented in our database. Hence, monthly

21 climatologies of [Chl-a] vertical profiles were computed for four geographical ~~points~~areas

22 (i.e. 4°x4° boxes) where the data density was high. These ~~points~~locations were also placed in

23 four main Mediterranean sub-basins (i.e. centered on 42°N/5°E in the North-Western basin,

24 38°N/5°E in the South-Western basin, 36°N/17°E in the Ionian Sea and 34°N/30°E in the

25 Levantine Sea, see yellow diamonds on Fig. 1). The monthly time-series are presented in the

26 next section (Sect. 3.1.1). Although, in the following, we refer to these time-series as

27 "climatological", certain average profiles result from a low number of fluorescence profiles

28 (sometimes less than 10, see numbers on Fig. 3) and therefore do not strictly represent a

29 climatological pattern. To better identify spatial changes in [Chl-a] fields, we also present

30 climatological transects (Sect. 3.1.2). Due to the weak density of data in the eastern basin, the

31 [Chl-a] distribution could only be analyzed along a 5°E north-south transect in the western

basin (see dotted line on Fig. 1). Nevertheless, this transect encompasses regions with different biological dynamics (D'Ortenzio and Ribera d'Alcalà, 2009) and it is representative of the main patterns of the Western Mediterranean.

3.1.1 Seasonality in four geographic ~~points~~locations

For each of the four selected geographic ~~points~~locations (see above), all available profiles in a 4°x4° side box centered on the chosen geographical position were averaged on a 1-meter vertical scale and on a monthly basis to produce climatological profiles. The resulting monthly climatologies are displayed on Fig. 3.

Overall, the climatological time-series representing the South-Western basin, the Ionian Sea and the Levantine Sea (Fig. 3, panels B, C and D) display a similar evolution of the vertical [Chl-a] distribution. From December to March, [Chl-a] is greater in the surface layer: from surface to the base of pycnocline (Fig. 2, panel B), while the April to November months are characterized by the occurrence of a DCM, concurrent with the development of the seasonal pycnocline close to surface. In the South-Western region, winter profiles present relatively high [Chl-a] in the upper meters ([Chl-a] > 0.5 mg m^{-3}), whereas in the Ionian, and even more in the Levantine, upper layer [Chl-a] is lower and the base of the pycnocline is deeper (about 150 m in the Ionian Sea and more than 200 m in the Levantine Sea). DCM, when occurring, is deeper in the Levantine and Ionian seas than in the South-Western region. The climatological time-series in the North-Western basin (Fig. 3, panel A) displays a different succession. DCM occurs from May to October, when surface stratification of the water column can be observed. In November and December, [Chl-a] vertical profiles display homogeneous concentrations from the surface to the upper limit of the pycnocline, which deepens through mixing processes. In January and February, the water density profiles are nearly constant and [Chl-a] profiles display low and homogeneous concentrations up to 100m. In March and April, although surface water density slightly decreases, pointing to water column stabilization and/or stratification, surface [Chl-a] considerably increases. Finally, all time-series are characterized by a deepening of the DCM from May to July and a shallowing from August to September. It appears that in the North-West region, the deepening of the DCM coincides with the deepening of the pycnocline. In the other areas, the pycnocline is much shallower than the DCM and their dynamics seem to be uncoupled until September. In October and November, the base of the surface mixed layer seems to be correlated with DCM.

1 Regarding [Chl-a] values, regional differences are visible, confirming previous observations

2 on the eastward increase of oligotrophic conditions. The highest [Chl-a] value is observed in

3 April, in the North-Western climatology (Fig. 3, panel A), reaching 1.2 mg m^{-3}. However, this

4 mean value is derived from extremely variable observations ranging between 0.3 and 4.2 mg

5 m^{-3}. The South-Western time-series shows [Chl-a] values up to 0.5 mg m^{-3}, observed in the

6 surface during winter and at the DCM during summer. In the Ionian climatology, highest

7 [Chl-a] values can be observed at the DCM, reaching 0.3 mg m^{-3}. Finally, the Levantine

8 climatology displays the lowest [Chl-a], with values rarely exceeding 0.25 mg m^{-3}.

9 Table 2 presents ~~averaged~~median [Chl-a] values at the DCM depth, for the four geographic

10 ~~points~~locations analyzed here. Contrary to the DCM [Chl-a] values visible in Fig. 3, the

11 values reported in Table 2 are derived from the ~~mean~~median DCM [Chl-a] values extracted

12 individually from each fluorescence profile presenting a DCM. In the North-Western region,

13 [Chl-a] at DCM is often around 1 mg m^{-3} , though it ranges between 0.~~65~~63 mg m^{-3} in

14 September and 1.~~22~~07 mg m^{-3} in April. At the South-Western point, the averaged [Chl-a] at

15 DCM is 0.~~87~~88 mg m^{-3}. In the Eastern basin, values are twice lower (about 0.55 mg m^{-3} at the

16 Ionian point and 0.~~45~~40 mg m^{-3} at the Levantine point). A seasonal pattern does not clearly

17 emerge from the analysis of the DCM statistics, except that [Chl-a] at DCM is generally

18 higher during spring and summer and lower during autumn. Note that ~~averaged~~median DCM

19 depth [Chl-a] values (Table 2) are higher than the DCM depth [Chl-a] values observed on

20 climatological profiles (Fig. 3) because the averaging process on the latter tends to ~~flat~~flatten

21 DCMs (see discussion on Sect. 4.1.2, Lavigne et al., 2012).

22 **3.2.1 North-South transect**

23 All the data located within ±2° from the 5°E meridian were selected to produce a

24 climatological pictures of [Chl-a] fields in spring (March to May, Fig. 4, panel A) and in

25 summer (June to September, Fig. 4, panel B).

26 The spring situation (Fig. 4, panel A) displays various types of profiles and a large range of

27 [Chl-a] values. North of 41°N, [Chl-a] values are high (> 1 mg m^{-3}) at surface and decrease

28 with depth. Highest [Chl-a] values (~3 mg m^{-3}) are observed around 42°N in surface (up to

29 30m depth). Between 40°N and 41°N, surface [Chl-a] is around 0.5 mg m^{-3} and a DCM is

30 visible at 50m depth. Further south, the climatological transect displays a deeper DCM

31 (around 75m depth) and very low surface [Chl-a] values (<0.3 mg m^{-3}).

1 In the summer transect (Fig. 4, panel B), the presence of a DCM is ubiquitous, although its
2 position in the water column and its [Chl-a] values vary throughout the transect. A steady
3 deepening of the DCM is observed from 43°N (DCM depth around 50 m) to 39°N (DCM
4 depth around 85 m). A southward decrease of [Chl-a] at DCM is also observed. It ranges from
5 0.8 mg m^{-3} to 0.4 mg m^{-3}. South of 39°N, a shallowing of the DCM depth and an increase of
6 the [Chl-a] at DCM are observed.

7 **3.2 Analysis of the profile shapes**

8 **3.2.1 Characteristics of standard shapes**

9 As a procedure was established to classify the shapes of the [Chl-a] profiles included in the
10 1994-2014 database (Sect. 2.3), certain characteristics related to [Chl-a] profiles could be
11 computed. They are summarized in Table 3.

12 ~~unsurprisingly,~~ MLD is shallowest when the standard vertical fluorescence shape is "DCM".
13 Additionally, the MLD is deepest when the standard florescence shape is "homogeneous". In
14 these 2 cases, the relative position of MLD and Z$_e$ confirm therefore that the "homogeneous"
15 and "DCM" shapes can be compared with the well-known "stratified" and "mixed" shapes
16 introduced by Morel and Berthon (1989). Profiles shapes categorized as "modified DCM",
17 "complex" and "HSC", display intermediate values for MLD. For profiles of the "modified
18 DCM" shape, the average distance between MLD and chlorophyll maxima is 22m. This
19 relatively short distance may indicate that the "modified DCM" shape derives from erosion by
20 deeper mixing of the DCM structure. For the "HSC" standard shape, MLD can be relatively
21 deep (ranging between 13m and 95m). A [Chl-a] gradient could therefore develop in both,
22 stratified and mixed conditions. According to Huisman et al., (1999), the development of a
23 [Chl-a] gradient in the mixed layer would be possible if mixed layer turbulence were low thus
24 allowing for the accumulation of phytoplankton cells near the surface.

25 According to the results presented in Table 3, ocean color surface [Chl-a] values are related to
26 the shape of the vertical profile. Lowest surface [Chl-a] values are observed for "DCM" shape
27 profiles while highest (~~1.22~~0.77 mg m^{-3}) values are observed for "HSC" shape profiles. In
28 spite of its variability, this high value suggests that the "HSC" shape could result from the
29 exponential growth of phytoplankton at surface in unlimited nutrient condition associated to a
30 stable water column. Hence, "HSC" profiles would typically correspond to bloom conditions.
31 A very high variability, with surface [Chl-a] values ranging from 0.13 mg m^{-3} to1.19 mg m^{-3},

14

is observed for profiles of the standard "homogenous" shape. This variability likely results from the interactions between the high variability of MLD and the recent development of phytoplankton biomass.

The F_{surf}/F_T ratio changes with the shape of the [Chl-a] profile. The lowest ratio (~~6~~5%) is observed for the "DCM" shape, even though this value is likely to be underestimated by a factor of 2.5 because of NPQ. The standard "~~homogeneous", "~~complex" and "HSC" shapes display similar ~~averaged~~median ratios, ~~32%, 30~~28% and ~~35~~31%, respectively. Once again, there is a large variability for "homogeneous" shape profiles that which can be explained by the variability of the MLD. Finally, in the "HSC" situation, the upper 20m can accumulate up to 50% of the chlorophyll content.

3.2.2 Seasonal distribution of the profile shapes

~~An objective~~A study of the seasonal distributions of standard shapes was performed for the main Mediterranean regions (Fig. 5, boundaries of the Mediterranean regions are drawn in the Fig. 1). During summer, all the regions are dominated by the "DCM" shape, with occurrences exceeding 90%. The "DCM" shape disappears in November everywhere, the time of its onset depends on the region: April for the Ionian, Levantine and Tyrrhenian regions, May for the South-West region and June for the North-West region. During the autumn/winter period, all the categories of shapes can be observed in one same region and during a same month. Nevertheless, profiles shapes classed as "modified DCM" are more frequent in early winter (i.e. the Ionian region where the "modified DCM" shape represents more than 60% of profiles in December and January), which reinforces the intuition that this shape might be generated by deeper mixing eroding the DCM structure. Profiles with the "homogeneous" shape are observed from November to March everywhere, except in the Ionian region. Similarly, the "complex" shape is present everywhere from November to March. Profiles displaying a "HSC" shape are absent, or nearly absent, in the Ionian and Levantine regions. In the Tyrrhenian and South-West regions, "HSC" profiles can be observed between November and March and are most abundant in February. In the North-West region, although "HSC" profiles are observed in winter, from November to February, they peak in spring (March – April) with occurrences exceeding 60%. Assuming that the "HSC" profiles denote bloom events, this result suggests that bloom events may occur during winter in the whole Western Mediterranean although they only peak in the North-West region during spring.

15

1 **3.2.3 Longitudinal and seasonal distribution of the DCM depth**

2 The DCM is confirmed to be a dominant feature of the [Chl-a] distribution in the

3 Mediterranean, although its characteristics change from one region to another and with time.

4 A deepening of the DCM depth with longitude is generally observed (Fig. 6), confirming

5 previous findings (Crise et al., 1999). A linear model applied to DCM depth data indicates

6 that, on average, DCM depth deepens by 1.6 m for 1° of longitude. However, a large

7 variability exists, especially in the Ionian and Levantine seas. Superimposed to this general

8 deepening of DCM with longitude, regional differences can be observed between the main

9 Mediterranean sub-basins. Considering profiles at the same range of longitude, the averaged

10 DCM depth is deeper and more variable in the South-West region than in the North-West

11 region (see Table 4). In the eastern basin, the Adriatic region displays shallow and stable

12 DCM depths, whereas the Ionian and Levantine regions display deeper and more variable

13 DCM depths (Table 4).

14 Part of the variability observed in the different Mediterranean regions can be explained by

15 seasonality. All the Mediterranean regions have a seasonal variability in the DCM depth (Fig.

16 7), which is characterized by a widespread deepening from March to mid-summer, and a

17 shallowing from mid-summer to November. In all the Mediterranean regions, except the

18 North-West region, there is 40% deepening of the DCM between spring and summer (33% in

19 the North-West).

20 **4   Discussion**

21 **4.1 Methodological discussion**

22 **4.1.1 Comparison with MEDATLAS**

23 The climatological profiles for each of the four geographical points analyzed in the Sect. 3.1

24 have been computed from the MEDATLAS climatology and compared to their fluorescence

25 based counterparts evaluated here (Fig. 8). For each geographical point, the two versions of

26 [Chl-a] vertical profiles (fluorescence based and MEDATLAS) displayed similar ranges of

27 values, although differences are observed in the form of [Chl-a] vertical profiles. The

28 fluorescence based profiles often display thinner DCMs with higher [Chl-a] values than in the

29 MEDATLAS climatology (see for instance Fig. 8, panel B summer, panel C autumn and

30 panel D summer). Moreover, in the MEDATLAS climatology, very weak seasonal changes of

the DCM depth are visible. These divergences can be explained by the use of discrete data and of interpolation in the MEDATLAS climatology, which prevents the proper characterization of vertical structures. In winter, the MEDATLAS climatology, and sometimes the fluorescence based climatology, show profiles with subsurface maxima (Fig. 8, panels A, B, C, winter), which have not been observed in the monthly fluorescence based time-series (Fig. 3). We hypothesize that these winter subsurface maxima could be an artifact caused by the large averaging timescale (from December to March), leading to the combination of [Chl-a] profiles with highly different vertical distributions (see Fig. 5). Another particular feature of the MEDATLAS climatology that does not show in the fluorescence-based climatology are the rises in summer and autumn surface [Chl-a] above DCM (Fig. 8, panels A, B and D). We suggest that this feature could result from the propagation by interpolation of the high surface [Chl-a] observed on coastal regions (see also Bosc et al., 2004). In addition, considering the geographical positions of the available MEDAR observations, in almost all the studied sub-basin (except Ionian) coastal observations are included in the database. They might therefore be responsible for the observed difference with the fluorescence-based climatology.

In summary, the results of this comparison demonstrate that, although the MEDATLAS database is extremely valuable, the derived MEDATLAS fields for [Chl-a] present serious limitations and they need to be updated.

4.1.2 Methodological approaches

In the present study, two different approaches have been used to describe the monthly variability of [Chl-a] profiles. On one hand, the "standard" method consists in averaging [Chl-a] values for a number of defined standard depths (i.e. Conkright et al., 2002, Sect. 3.1). On the other hand, a "probabilistic" method (Sect. 3.2), for which each [Chl-a] profile is considered as a whole, focuses the analysis on its general shape and on specific features (e.g. DCM depth). The second approach requires an *a priori* knowledge of the different profile shapes found in the database as well as the definition of an efficient and automatic procedure to categorize the profiles. In this ~~study~~analysis, the main standard shapes and the classification procedure were defined after individual visualization of all the fluorescence profiles in the database and determination of their characteristics (i.e. D_{max}, F_{MLD}/F_T, F_{max}/F_{surf}, see Sect. 2.3 for details).

1   The two approaches are complementary. The "standard" method highlights the average
2   pattern of the [Chl-a] profile and provides the ranges of [Chl-a] values. However, [Chl-a]
3   values must be considered independently for each depth and the shape of the resulting
4   climatological profile has to be interpreted carefully because it is a composite. A typical
5   artifact of this method is the tendency of the DCM to be flattened (compare DCM of Fig. 3
6   and values of Table 2). In these cases (i.e. [Chl-a] profile extremely stable, as during summer,
7   or very dynamic, as during winter), the "probabilistic" analysis of the shape of the [Chl-a]
8   profile appears more pertinent. In addition, the "probabilistic" analysis provides information
9   on the environmental processes that lead to the observed [Chl-a] shape. As mentioned in Sect.
10 3.2.1, the "modified DCM" shape likely results from the erosion by upper vertical mixing of
11 the DCM structure while the "homogenous" standard shape is likely driven by vertical
12 mixing, which encompasses the whole [Chl-a] profile. Similarly, the "HSC" profiles,
13 associated to high surface [Chl-a] values (see Table 3), could be collected (and then
14 associated) to surface phytoplankton bloom conditions. Under these conditions, if there is no
15 nutrient limitation, growth rate is essentially affected by light availability and then decreases
16 with depth. This can account for the derived decrease in the [Chl-a] gradient from surface to
17 depth. Nevertheless, these conjectures have to be considered on a statistical basis. Indeed,
18 each individual profile is affected by complex and variable factors (i.e. vertical mixing, 3D
19 dynamic structures, light distribution, grazing pressure, Longhurst and Harrison, 1989, see
20 also discussion below), which sometimes lead to erratic [Chl-a] vertical distributions that
21 become difficult to explain (17% of profiles have been classed as "complex" standard
22 shapes). Finally, the "probabilistic" analysis also revealed that seasonal changes in [Chl-a]
23 profiles are not smooth and steady, as the climatological analysis may suggest, but are rather
24 ~~strongly dynamic.~~extremely variable.

25 **4.2 A new vision of the [Chl-a] in the Mediterranean Sea**

26 **4.2.1 Comparison with satellite ocean color observations**

27 The main feature that emerges from the analysis of annual cycles of surface [Chl-a] from
28 ocean color data over the Mediterranean sea is the coexistence of two main types of cycle
29 (Bosc et al., 2004; D'Ortenzio and Ribera 2009; Lavigne et al., 2013). The two cycles ("NO
30 BLOOM" and "BLOOM", following the definition of D'Ortenzio and Ribera d'Alcalà, 2009)
31 can be characterized, firstly, by a two-fold increase from summer to winter in the normalized
32 [Chl-a] (so-called NO BLOOM annual cycle) and secondly, by a moderate (two-fold) increase

in normalized [Chl-a] from summer to winter, followed by an exponential increase (three-fold) in early spring (so-called BLOOM annual cycle). These previous findings are based on satellite surface [Chl-a] and result from a complex statistical analysis (i.e. normalization of the seasonal cycles, clustering analysis), but they have also been confirmed by the climatological time-series presented here (see Sect. 3.1). Climatologies of [Chl-a] profiles (Fig. 3) for the South-Western region (panel B), the Ionian region (panel C) and the Levantine region (panel D), which correspond to the NO BLOOM regions identified by D'Ortenzio and Ribera d'Alcalà (2009), display similarities in the seasonal variations of surface [Chl-a] and they also showed a similar succession of winter homogeneous profiles and summer profiles with DCM. In contrast, the time-series corresponding to the North-Western region (Fig. 3, panel A) presents, in March and April, [Chl-a] vertical profiles characterized by high surface concentrations (i.e. HSC profiles), confirming the specific feature of the North-Western region in the Mediterranean Sea. Unlike NO BLOOM Mediterranean regions, in the North-West region, the average winter MLD is deeper than the DCM and the nitracline depth (see Table 4). This particularity explains the March-April bloom, which could be supported by large winter nutrient supplies, and/or the dilution of grazers. It also indicates that winter vertical mixing fully destroys the nitracline, pycnocline and DCM, which have to be restored each year. The annual renewal of these structures contributes to their tight coupling (see Fig. 3 panel A and Table 4), which is not observed in NO BLOOM Mediterranean regions (based on Fig. 3 results, DCM and pycnocline are uncoupled). In NO BLOOM regions, DCM and nitracline are not reached by the average winter MLD (see Table 4) except for extreme MLD events (Lavigne et al., 2013), winter MLD does not generally reach the depths of reached by DCM and nitracline during summer (see Table 4).

Beyond the bimodal conception (i.e. BLOOM / NO BLOOM) of annual [Chl-a] cycles in the Mediterranean Sea, there is an important and unresolved complexity marked by the presence of regional differences within the two main biomass annual cycles. A good illustration of this complexity is the identification by D'Ortenzio and Ribera d'Alcalà (2009) of three different annual cycles (i.e. 3 bioregions) for the NO BLOOM dynamics. The probabilistic analysis of the general shape of the [Chl-a] profiles achievedperformed in this paper also contributes to refine the basic BLOOM / NO BLOOM scheme and should help to explain the complex patterns observed from the surface. In Fig. 5, regional differences in the distribution of the standard shapes for [Chl-a] vertical profiles are observed among the NO BLOOM regions (i.e. South-West, Levantine and Ionian regions). The main difference is the significant proportion

1   of "HSC" like profiles during winter months (i.e. January, February and March) in the South-
2   West region, whereas this proportion is very small (less than 10%) in the Ionian sea, and even
3   zero in the Levantine Sea. The observation of "HSC" like profiles in the South-West region
4   suggests that, during winter, mixing is able to supply enough nutrients at the surface to
5   support episodic developments of phytoplankton close to the surface, when water column
6   begins to stabilize. This could also explain the higher [Chl-a] observed in the South-West
7   region and the difference between the South-Western and Eastern normalized [Chl-a] annual
8   cycles (D'Ortenzio and Ribera d'Alcalà, 2009). Compared to the Eastern Mediterranean Sea,
9   DCM and nitracline depths are shallow in the South-West region (Table 4). However, winter
10 mixing is constrained, in the Algerian basin, by the strong halocline associated to the
11 spreading of Atlantic Water, and barely reaches the nitracline depth (D'Ortenzio and Prieur,
12 2010; Lavigne et al., 2013). ~~Therefore,~~As 3-D sub-mesoscale activity, associated to jets,
13 fronts and eddies, is also similarly intense in both, South-Western and Eastern basins (Rio et
14 al., 2007), our best explanation for the spatial divergences in the occurrence of "HSC" profiles
15 ~~might originate in~~is the regional differences in nutrient stocks below the nitracline. Indeed, for
16 the intermediate layer, the nitrate concentration is much higher in the Western than in the
17 Eastern basin (Ribera d'Alcalà et al., 2003). In addition, the nitrate to phosphate ratio
18 increases eastward, suggesting that phytoplankton growth is mainly limited by phosphate in
19 the Eastern Mediterranean Sea (Ribera d'Alcalà et al., 2003, Bethoux et al., 2002; Krom et al.,
20 1991). Hence, the absence of "HSC" profiles in the Eastern Mediterranean Sea could be due
21 to a too weak mixing efficiency to supply sufficient amounts of nitrate and phosphate for
22 supporting a phytoplankton bloom.

23 **4.2.2 High diversity of the Mediterranean [Chl-a]**

24 Although the Mediterranean Sea covers a relatively small latitudinal range (from 30°N to
25 45°N), previous findings, essentially based on satellite observations, have shown that in this
26 basin, the annual phytoplankton cycles representative of subtropical and mid-latitude regions
27 of the global ocean coexist (D'Ortenzio and Ribera d'Alcalà 2009, Lavigne et al., 2013).
28 Present results, which focus on the seasonal variability of the whole [Chl-a] vertical
29 distribution, confirm these previous statements. The climatological time-series of [Chl-a]
30 profiles (Fig. 3) for the South-Western region (panel B), the Ionian region (panel C) and the
31 Levantine region (panel D) are very close to typical subtropical behavior marked by the quasi-
32 permanent existence of the DCM (Letelier et al., 2004; Mignot et al., 2014). In particular, the
33 [Chl-a] climatology of the BATS station in the subtropical North Atlantic gyre (Steinberg et

al., 2001; Lavigne et al., 2012) displays many similarities, in terms of ranges of values for [Chl-a], DCM depths and winter mixing depths, with the climatological time-series built in the Levantine Sea (Fig. 3, panel D). The only main difference is that the "homogeneous" climatological profiles begin in December in the Mediterranean regions and only in January at the BATS station (Lavigne et al., 2012). Regarding seasonal cycles obtained for the North-Western Mediterranean Sea, they can be easily compared to mid-latitude (40°-60°) regions marked by an intense spring bloom as in the North Atlantic (Siegel et al., 2002) or in certain regions of the Southern Ocean (Thomalla et al., 2011). Similarly to our northwestern Mediterranean observations, the seasonal cycles for [Chl-a] vertical profiles presented by Boss et al. (2008) in the Western North-Atlantic (about 50°N) and by Chiswell (2011) in the waters east of New Zealand (about 40°S) display a majority of profiles with a "homogeneous" shape during winter and, in spring, a predominance of profiles displaying a "HSC" shape or an "homogeneous" shape with high [Chl-a] values. The coexistence of profiles with "homogeneous" and "HSC" shapes during spring could be explained by the intermittent feature of mixing, which continuously modifies the vertical distribution of [Chl-a] during the spring bloom (Chiswell, 2011). Finally, it is important to mention that the summer situation is very different between the North-Atlantic region studied by Boss et al. (2008) and the North-Western Mediterranean Sea. Although, DCM like profiles are nearly permanent in the North-Western Mediterranean from May/June, Boss et al. (2008) only observed them to start in late summer.

The present study also shows that in the Mediterranean Sea, the specific features of the [Chl-a] profiles with a "DCM" shape have a large variability, comparable to those observed in the Global ocean, although occurring on shorter spatial scales. The most relevant indicator is certainly the DCM depth, which was observed to range between 30m and more than 150m. As expected (e.g. Cullen, 2015), the depth of the Mediterranean DCM is inversely related to the surface [Ch-a] (Fig. 9). In addition, the relationship between the DCM depth and surface [Chl-a] (blue curve on Fig. 9) is similar to the relationship reported for the Global ocean (red curve on Fig. 9, Mignot et al., 2011). This observation suggests that certain DCM properties in the Mediterranean Sea conform to the same generic properties established for the Global Ocean.

At the first order, the DCM depth variability in the Mediterranean Sea is related to the spatial component and, in particular, longitude. The deepening of the DCM along a longitudinal gradient (in the present study, DCM deepens by 1.6m per 1 degree of longitude east) agrees with the previous review, also based on observations, by Crise et al. (1999). This general

21

1 deepening of the DCM with longitude covaries with the eastward increase of oligotrophy in

2 the Mediterranean Sea (Béthoux et al., 1998). This pattern is generally attributed to anti-

3 estuarine circulations in the Straits of Gibraltar and Sicily, which generate an eastward inflow

4 of surface nutrient depleted waters and a westward outflow of deep nutrient rich waters. In the

5 Eastern Mediterranean Sea, oligotrophy is also maintained by poor nutrient inputs from the

6 boundaries (atmosphere and coasts) and by the formation of Levantine Intermediate Water,

7 which is not the product of deep convection but of the subduction of surface water into

8 intermediate water layers (Robinson and Golnaraghi). As revealed by Table 4, regional

9 changes in DCM depth, nitracline depth and averaged daily PAR at DCM are correlated in the

10 Mediterranean Sea. The eastward deepening of the DCM depth and of the nitracline depth is

11 accompanied by a decrease in the mean daily averaged PAR at DCM (values ranging from 1

12 mol quanta m^{-2} day^{-1} in the North-West Mediterranean to 0.16 mol quanta m^{-2} day^{-1} in the

13 Levantine Sea). This trend concurs with the ''general rule'' that states that the DCM builds-up

14 where there is an optimal balance between the upward nutrient flux and the downward photon

15 flux and lies on top of the nutricline (Cullen, 2015). The large distance between DCM depth

16 and nitracline depth in the Ionian (36m) and the Levantine (83m) basins may be considered as

17 contradictory with the previous theory. However, according to Table 4, the estimations of

18 nitracline depths are not likely to be good estimators of the top of the nitracline, if the nitrate

19 gradient is not ~~a~~sharp enough ~~sharp feature~~, as is it the case, for example in the Eastern

20 Mediterranean Sea. Indeed, nitracline depths have been computed from discrete vertical

21 profiles, using the 1µM isoline (Lavigne et al., 2013).

22 Results from Fig. 10 also show that a seasonal component contributes to explain DCM

23 variability in the Mediterranean regions. The observed seasonal pattern of the DCM depth

24 (i.e. deepening from spring to summer and shallowing from summer to autumn) is consistent

25 with previous model results (Macias et al., 2014), and with individual Bio-Argo float

26 observations (Mignot et al., 2014). Letelier et al. (2004) and Mignot et al. (2014) explain this

27 seasonal pattern by considering that the DCM depth might be driven by the light availability

28 and that it would follow the depth of an isolume. This observation is confirmed here by the

29 analysis of the vertical [Chl-a] profile as a function of irradiance for the spring, summer and

30 autumn periods (Fig. 10). For all regions, from spring to summer, PAR at DCM depth

31 remains unchanged although [Chl-a] decreases. Accordingly to Letelier et al. (2004), higher

32 spring [Chl-a] may be explained by the temporal erosion of the upper nitracline from spring to

1 summer, supporting the hypothesis of deep biomass maxima. From summer to autumn, the

2 magnitude of DCMs remains roughly unchanged, similarly to the PAR at DCM.

3 **5   Conclusion**

4 Since the initial work of the MEDAR/MEDATLAS group (Maillard and coauthors, 2005;

5 Manca et al., 2004), the proposed study represents the first attempt to analyze the seasonal

6 variations of the [Chl-a] vertical distribution over the Mediterranean Sea. The picture of the

7 [Chl-a] field in the basin has been updated here, as it had been mainly derived from surface

8 satellite data or from limited and scarce in situ observations. Chlorophyll-a fluorescence data

9 (specifically calibrated and ~~homogenized~~consistently processed with a dedicated method)

10 provided a significantly larger database than the commonly used in situ bottle estimations.

11 Additionally, a better description of the vertical distribution was made possible. 6790 profiles

12 of fluorescence were gathered and processed to carry out a comprehensive analysis of the

13 seasonal variability of the vertical [Chl-a] profiles within the main Mediterranean sub-basins.

14 The present analysis, in agreement with previous satellite results (D'Ortenzio and Ribera

15 d'Alcalà, 2009), demonstrates the coexistence of two main types of dynamics (i.e. subtropical

16 and mid-latitude dynamics) in the Mediterranean Sea. Mid-latitude dynamics are observed in

17 the North-Western basin. Their main specificity is the high occurrence of "HSC" profiles in

18 March and April, whereas this type of shape, associated to bloom conditions, is nearly absent

19 elsewhere during this season. The subtropical dynamics encompass most of the remaining

20 basin. It is characterized by an omnipresent DCM from spring to autumn and by a large

21 variety of [Chl-a] vertical shapes during winter. The present analysis also demonstrated that

22 the [Chl-a] pattern in the Mediterranean Sea is not uniform. Even among regions with

23 subtropical dynamics, a strong variability was observed in [Chl-a] values or DCM

24 characteristics. At the basin scale, this variability follows an eastward oligotrophic pattern.

25 The present study was often limited by the quantity of data, which did not allow for the

26 analysis of each region of the Mediterranean Sea (e.g. the Adriatic Sea). We regret the

27 singular absence of fluorescence profiles in oceanographic databases compared to other

28 parameters. For instance, in the MEDAR database, there are 118009 salinity profiles, 44928

29 oxygen profiles and only 1984 chlorophyll-a fluorescence profiles. Finally, in this study we

30 were only able to present climatological behaviors. Although it is a first and necessary step

31 for a better understanding of processes which impact seasonal variability of [Chl-a] vertical

32 profiles, it would be interesting to further study certain particular cases showing, with a high

23

frequency, annual series of vertical [Chl-a] profiles. These data have now become available with the development of Bio-Argo floats (Johnson et al., 2009) and some studies have already demonstrated their potential for such applications (Boss and Behrenfeld, 2010; Mignot et al., 2014).

Acknowledgements

References

Andersen, V., and Prieur, L.: One-month study in the open nw mediterranean sea (dynaproc experiment, may 1995): overview of the hydrobiogeochemical structures and effects of wind events, Deep Sea Research Part I: Oceanographic Research Papers, 47(3):397–422, 2000.

Antoine, D., Morel, A., and André, J.-M.: Algal pigment distribution and primary production in the eastern Mediterranean as derived from coastal zone color scanner observations, Journal of Geophysical Research, 100, PP. 16,193–16,209, doi: 199510.1029/95JC00466, 1995.

Barale, V., Jaquet, J.-M., and Ndiaye, M.: Algal blooming patterns and anomalies in the Mediterranean Sea as derived from the SeaWiFS data set (1998-2003), Remote Sensing of Environment, 112, 3300–3313, doi: 10.1016/j.rse.2007.10.014, 2008.

1 Béthoux, J., Morin, P., Chaumery, C., Connan, O., Gentili, B., and Ruiz-Pino, D.: Nutrients in
2 the Mediterranean Sea, mass balance and statistical analysis of concentrations with respect to
3 environmental change, Marine Chemistry, 63, 155–169, doi: 10.1016/S0304-4203(98)00059-
4 0, 1998.

5 Béthoux, J. P., Morin, P., and Ruiz-Pino, D. P.: Temporal trends in nutrient ratios: chemical
6 evidence of Mediterranean ecosystem changes driven by human activity, Deep Sea Research
7 Part II: Topical Studies in Oceanography, 49, 2007–2016, doi: 10.1016/S0967-
8 0645(02)00024-3, 2002.

9 Biermann, L., Guinet, C., Bester, M., Brierley, A., and Boehme, L.: An optimised method for
10 correcting quenched fluorescence yield, Ocean Science Discussions, 11, 1243–1264, 2014.

11 Bosc, E., Bricaud, A., and Antoine, D.: Seasonal and interannual variability in algal biomass
12 and primary production in the Mediterranean Sea, as derived from 4 years of SeaWiFS
13 observations, Global Biogeochemical Cycles, 18, 2004.

14 Boss, E. and Behrenfeld, M.: In situ evaluation of the initiation of the North Atlantic
15 phytoplankton bloom, Geophysical Research Letters, 37, doi: 10.1029/2010GL044174, 2010.

16 Boss, E., Swift, D., Taylor, L., Brickley, P., Zaneveld, R., Riser, S., Perry, M., and Strutton,
17 P.: Observations of pigment and particle distributions in the western North Atlantic from an
18 autonomous float and ocean color satellite, Limnology and Oceanography, 53, 2112–2122,
19 doi: 10.4319/lo.2008.53.5_part_2.2112, 2008.

20 Boyer, T. P., Antonov, J. I., Baranova, O. K., Carla, C., Garcia, H. E., Grodsky, A., Johnson,
21 D. R., Locarnini, R. A., Mishonov, A. V., O'Brien, T. D., Paver, C. R., Reagan, J. R., Seidov,
22 D., Smolyar, I. V., and Zwengan, M. M.: World Ocean Database 2013, Sydney Levitus, Ed.;
23 Alexey Mishonov, Technical Ed.; NOAA Atlas NESDIS 72, 209 pp, 2013.

24 Casotti, R., Landolfi, A., Brunet, C., D'Ortenzio, F., Mangoni, O., Ribera d'Alcalà, M., and
25 Denis, M.: Composition and dynamics of the phytoplankton of the Ionian Sea (eastern
26 Mediterranean), Journal of Geophysical Research: Oceans (1978–2012), 108, 2003.

27 Cetinic, I., Toro-Farmer, G., Ragan, M., Oberg, C., and Jones, B.: Calibration procedure for
28 Slocum glider deployed optical instruments, Optics Express, 17, 15420–15430, 2009.

25

Chiswell, S.: Annual cycles and spring blooms in phytoplankton: don't abandon Sverdrup completely, MEPS, 443, 39-50, 2011.

Christaki, U., Giannakourou, A., Van Wambeke, F., and Grégori, G.: Nanoflagellate predation on auto-and heterotrophic picoplankton in the oligotrophic Mediterranean Sea, Journal of Plankton Research, 23, 1297–1310, 2001.

Claustre, H., Fell, F., Oubelkheir, K., Prieur, L., Sciandra, A., Gentili, B., and Babin, M.: Continuous monitoring of surface optical properties across a geostrophic front: Biogeochemical inferences: Limnology and oceanography, 45(2):309–321, 2000.

Claustre, H., Hooker, S.B., Van Heukelem, L., Berthon, J-F., Barlow, R., Ras, J., Sessions, S., Targa, C., Thomas, C. S., van der Linde, D. et al.: An intercomparison of hplc phytoplankton pigment methods using in situ samples: application to remote sensing and database activities, Marine Chemistry, 85(1):41–61, 2004.

Conkright, M., O'Brien, T., Stephens, K., Locarnini, R., Garcia, H., Boyer, T., and Antonov, J.: World Ocean Atlas 2001, Volume 6: Chlorophyll, Ed. S. Levitus, NOAA Atlas NESDIS 54, U.S. Governement Printing Office, Wash., D.C., 46 pp., 2002.

Crise, A., Allen, J., Baretta, J., Crispi, G., Mosetti, R., and Solidoro, C.: The Mediterranean pelagic ecosystem response to physical forcing, Progress In Oceanography, 44, 219–243, doi: 10.1016/S0079-6611(99)00027-0, 1999.

Crombet, Y., Leblanc, K., Queguiner, B., Moutin, T., Rimmelin, P., Ras, J., Claustre, H., Leblond, N., Oriol, L., and Pujo-Pay, M.: Deep silicon maxima in the stratified oligotrophic Mediterranean Sea., Biogeosciences, 8, 459–475, 2011.

Cullen, J.: The Deep Chlorophyll Maximum - Comparing Vertical Profiles of Chlorophyll-A, Canadian Journal of Fisheries and Aquatic Sciences, 39, 791–803, 1982.

Cullen, J. J.: Subsurface chlorophyll maximum layers: enduring enigma or mystery solved?, Annual review of marine science, 7, 207–239, 2015.

Cullen, J. and Lewis, M.: Biological Processes and Optical Measurements Near the Sea Surface: Some Issues Relevant to Remote Sensing, Journal of Geophysical Research-Oceans, 100, 13255–13266, 1995.

1   de Boyer Montegut, C., Madec, G., Fischer, A., Lazar, A., and Iudicone, D.: Mixed layer

2   depth over the global ocean: An examination of profile data and a profile-based climatology,

3   Journal of Geophysical Research-Oceans, 109, doi: 10.1029/2004JC002378, 2004.

4   Devred, E., Sathyendranath, S., and Platt, T.: Delineation of ecological provinces using ocean

5   colour radiometry, Marine Ecology Progress Series, 346, 1–13, 2007.

6   Dolan, J., Vidussi, F., and Claustre, H.: Planktonic ciliates in the Mediterranean Sea:

7   longitudinal trends, Deep Sea Research Part I: Oceanographic Research Papers, 46, 2025–

8   2039, doi: 10.1016/S0967-0637(99)00043-6, 1999.

9   Dolan, J., Claustre, H., Carlotti, F., Plounevez, S., and Moutin, T.: Microzooplankton

10   diversity: relationships of tintinnid ciliates with resources, competitors and predators from the

11   Atlantic Coast of Morocco to the Eastern Mediterranean, Deep Sea Research Part I:

12   Oceanographic Research Papers, 49, 1217–1232, doi: 10.1016/S0967-0637(02)00021-3,

13   2002.

14   D'Ortenzio, F. and Ribera d'Alcalà , M.: On the trophic regimes of the Mediterranean Sea: a

15   satellite analysis, Biogeosciences, 6, 139–148, doi: 10.5194/bg-6-139-2009, 2009.

16   D'Ortenzio, F. and Prieur, L.: The upper mixed layer, Life in the Mediterranean Sea: A look

17   at habitat changes, edited by: Noga Stambler, Nova Science Publisher, pp. 127–156, 2012.

18   D'Ortenzio, F., Iudicone, D., Montegut, C., Testor, P., Antoine, D., Marullo, S., Santoleri, R.,

19   and Madec, G.: Seasonal variability of the mixed layer depth in the Mediterranean Sea as

20   derived from in situ profiles, Geophysical Research Letters, 32, doi: 10.1029/2005GL022463,

21   2005.

22   D'Ortenzio, F., Thierry, V., Eldin, G., Claustre, H., Testor, P., Coatanoan, C., Tedetti, M.,

23   Guinet, C., Poteau, A., Prieur, L., et al.: White Book on Oceanic Autonomous Platforms for

24   Biogeochemical Studies: Instrumentation and Measure (PABIM) version 1.3, [online]

25   Available from: http://www.obs-vlfr.fr/OAO/file/PABIM_white_book_version1.3.pdf, 2010.

26   D'Ortenzio, F., Lavigne, H., Besson, F., ClaLavigne, H., Coppola, L., Garcia, N., Laes-Huon,

27   A.s-Huon, A., Le Reste, S., Malardé, D., Migon, C., et al.: Observing mixed layer depth,

28   nitrate and chlorophyll concentrations in the northwestern Mediterranean: A combined

29   satellite and NO3 profiling floats experiment, Geophysical Research Letters, 2014.

Dugdale, R. and Wilkerson, F.: Nutrient sources and primary production in the Eastern Mediterranean, Oceanol. Acta, 9, 179–184, 1988.

Durrieu de Madron, X., Guieu, C., Sempéré, R., Conan, P., Cossa, D., D'Ortenzio, F., Estournel, C., Gazeau, F., Rabouille, C., Stemmann, L., et al.: Marine ecosystems responses to climatic and anthropogenic forcings in the mediterranean, Progress in Oceanography, 91(2):97–166, October 2011.

Estrada, M., Marrase, C., Latasa, M., Berdalet, E., Delgado, M., and Riera, T.: Variability of deep chlorophyll maximum characteristics in the Northwestern Mediterranean, Marine Ecology-Progress Series, 92, 289-289, 1993.

Feldman, G., Kuring, N., Ng, C., Esaias, W., McClain, C., Elrod, J., Maynard, N., and Endres, D.: Ocean-color: availability of the global data set, EOS, p. 634, 1989.

Franz, B., Werdell, P., Meister, G., Bailey, S., Eplee, R., Feldman, G., Kwiatkowskaa, E., McClain, C., Patt., F., and Thomas, D.: The continuity of ocean color measurements from SeaWiFS to MODIS, in J.J. Butler (Ed.), Earth observing systems: X. Proceedings SPIE, vol. 5882, The International Society for Optical Engineering, pp. 1-13, 2005.

Gieskes, W. W. and Kraay, G. W.: Unknown Chlorophyll a Derivatives in the North Sea and the Tropical Atlantic Ocean Revealed by HPLC Analysis, Limnology and Oceanography, 28, 757–766, 1983.

Huisman, J., Oostveen, P. v., and Weissing, F. J.: Critical Depth and Critical Turbulence: Two Different Mechanisms for the Development of Phytoplankton Blooms, Limnology and Oceanography, 44, 1781–1787, 1999.

Ignatiades, L., Gotsis-Skretas, O., Pagou, K., and Krasakopoulou, E.: Diversification of phytoplankton community structure and related parameters along a large-scale longitudinal east-west transect of the Mediterranean Sea, Journal of Plankton Research, 31, 411-428, 2009.

Johnson, K. S., Berelson, W. M., Boss, E. S., Chase, Z., Claustre, H., Emerson, S. R., Gruber, N., Kortzinger, A., Perry, M. J., and Riser, S. C.: Observing biogeochemical cycles at global scales with profiling floats and gliders: Prospects for a global array, Oceanography, 22, 216–225, 2009.

Kiefer, D.A.: Fluorescence properties of natural phytoplankton populations, Mar.Biol., 22, 263-269, 1973.

Kolber, Z. and Falkowski, P. G.: Use of Active Fluorescence to Estimate Phytoplankton Photosynthesis in Situ, Limnology and Oceanography, 38, 1646–1665, 1993.

Krom, M. D., Kress, N., Brenner, S., and Gordon, L. I.: Phosphorus Limitation of Primary Productivity in the Eastern Mediterranean Sea, Limnology and Oceanography, 36, 424–432, 1991.

Krom, M., Brenner, S., Kress, N., Neori, A., and Gorgon, L.: Nutrient Dynamics and New Production in a Warm-Core Eddy from the Eastern Mediterranean-Sea, Deep-Sea Research Part A, 39, 467–480, 1992.

Lavigne, H., D'Ortenzio, F., Claustre, H., and Poteau, A.: Towards a merged satellite and in situ fluorescence ocean chlorophyll product, Biogeosciences, 9, 2111–2125, 2012.

Lavigne, H., D'Ortenzio, F., Migon, C., Claustre, H., Testor, P., d'Alcalà, M. R., Lavezza, R., Houpert, L., and Prieur, L.: Enhancing the comprehension of mixed layer depth control on the Mediterranean phytoplankton phenology, Journal of Geophysical Research: Oceans, 118, 3416–3430, doi: 10.1002/jgrc.20251, 2013.

Letelier, R. M., Karl, D. M., Abbott, M. R., and Bidigare, R. R.: Light Driven Seasonal Patterns of Chlorophyll and Nitrate in the Lower Euphotic Zone of the North Pacific Subtropical Gyre, Limnology and Oceanography, 49, 508–519, 2004.

Longhurst, A. R.: Ecological Geography of the Sea, Second Edition, Academic Press, 2 edn., 2006.

Longhurst, A. R. and Harrison, G. W.: The biological pump: profiles of plankton production and consumption in the upper ocean, Progress in Oceanography, 22, 47–123, 1989.

Lorenzen, C. J.: A method for the continuous measurement of in vivo chlorophyll concentration, Deep-Sea Research, 13, 223–227, 1966.

Macias, D., Stips, A., and Garcia-Gorriz, E.: The relevance of deep chlorophyll maximum in the open Mediterranean Sea evaluated through 3D hydrodynamic-biogeochemical coupled simulations, Ecological Modelling, 281, 26–37, 2014.

1 Maillard, C. and Coauthors: MEDAR/MEDATLAS 1998-2001: A Mediterranean and Black

2 Sea oceanographic data base and network, 46, 329–344, 2005.

3 Manca, B., Burca, M., Giorgetti, A., Coatanoan, C., Garcia, M.-J., and Iona, A.: Physical and

4 biochemical averaged vertical profiles in the Mediterranean regions: an important tool to trace

5 the climatology of water masses and to validate incoming data from operational

6 oceanography, Journal of marine systems, 48, 83–116, 2004.

7 Marty, J.-C., Chiaverini, J., Pizay, M.-D., and Avril, B.: Seasonal and interannual dynamics of

8 nutrients and phytoplankton pigments in the western Mediterranean Sea at the DYFAMED

9 time-series station (1991-1999), Deep Sea Research Part II, 49, 1965–1985, doi: 16/S0967-

10 0645(02)00022-X, 2002.

11 McClain, C., Cleave, M., Feldman, G., Gregg, W., Hooker, S., and Kuring, N.: Science

12 quality SeaWiFS data for global biosphere research, Sea Technology, 39, 10–16, 1998.

13 Mignot, A., Claustre, H., D'Ortenzio, F., Xing, X., Poteau, A., and Ras, J.: From the shape of

14 the vertical profile of in vivo fluorescence to Chlorophyll-a concentration, Biogeosciences, 8,

15 2391–2406, doi: 10.5194/bg-8-2391-2011, 2011.

16 Mignot, A., Claustre, H., Uitz, J., Poteau, A., D'Ortenzio, F., and Xing, X.: Understanding the

17 seasonal dynamics of phytoplankton biomass and the deep chlorophyll maximum in

18 oligotrophic environments: A Bio-Argo float investigation, Global Biogeochemical Cycles,

19 28, 856–876, 2014.

20 Muller, P., Li, X.-P., and Niyogi, K. K.: Non-Photochemical Quenching. A Response to

21 Excess Light Energy, Plant Physiology, 125, 1558 –1566, doi: 10.1104/pp.125.4.1558, 2001.

22 Morel, A. and André, J.-M.: Pigment Distribution and Primary Production in the Western

23 Mediterranean as Derived and Modeled From Coastal Zone Color Scanner Observations,

24 Journal of Geophysical Research, 96, PP. 12,685–12,698, doi: 199110.1029/91JC00788,

25 1991.

26 Morel, A. and Berthon, J.: Surface Pigments, Algal Biomass Profiles, and Potential

27 Production of the Euphotic Layer - Relationships Reinvestigated in View of Remote-Sensing

28 Applications, Limnology and Oceanography, 34, 1545–1562, 1989.

Morel, A. and Maritorena, S.: Bio-optical properties of oceanic waters: A reappraisal, Journal of Geophysical Research-Oceans, 106, 7163–7180, 2001.

Moutin, T. and Raimbault, P.: Primary production, carbon export and nutrients availability in western and eastern Mediterranean Sea in early summer 1996 (MINOS cruise), Journal of Marine Systems, 33-34, 273–288, doi: 10.1016/S0924-7963(02)00062-3, 2002.

Moutin, T. and Prieur, L.: Influence of anticyclonic eddies on the Biogeochemistry from the Oligotrophic to the Ultraoligotrophic Mediterranean (BOUM cruise), Biogeosciences, 9, 3827–3855, doi: 10.5194/bg-9-3827-2012, 2012.

Moutin, T., Van Wambeke, F., and Prieur, L.: Introduction to the Biogeochemistry from the Oligotrophic to the Ultraoligotrophic Mediterranean (BOUM) experiment, Biogeosciences, 9, 3817-3825, 2012.

Navarro, G., Vázquez, Á., Macás, D., Bruno, M., and Ruiz, J.: Understanding the patterns of biological response to physical forcing in the Alborán Sea (western Mediterranean), Geophysical Research Letters, 38, 2011.

Platt, T., Sathyendranath, S., White III, G. N., Fuentes-Yaco, C., Zhai, L., Devred, E., and Tang, C.: Diagnostic properties of phytoplankton time series from remote sensing, Estuaries and Coasts, 33, 428–439, 2010.

Psarra, S., Tselepides, A., and Ignatiades, L.: Primary productivity in the oligotrophic Cretan Sea (NE Mediterranean): seasonal and interannual variability, Progress in Oceanography, 46, 187–204, 2000.

Rio M.-H., Poulain P.-M., Pascual A., Mauri, E., Larnicol, G., and Santoleri, R.: A mean dynamic topography of the Mediterranean Sea computed from altimetric data, in-situ measurements and a general circulation model, Journal of Marine Systems, 65, 484-508, 2007.

Robinson, A. and Golnaraghi, M.: The physical and dynamical oceanography of the Mediterranean Sea, in: Ocean processes in climate dynamics: Global and Mediterranean examples, vol. 419 of NATO Science Series, p. 255-306, springerlink edn., 1994.

Rottgers, R. and Koch, B. P.: Spectroscopic detection of a ubiquitous dissolved pigment degradation product in subsurface waters of the global ocean, Biogeosciences, 9, 2585-2596, 2012.

Sackmann, B., Perry, M., and Eriksen, C.: Seaglider observations of variability in daytime fluorescence quenching of chlorophyll-a in Northeastern Pacific coastal waters, Biogeosciences Discussions, 5, 2839–2865, 2008.

Sharples, J., Moore, C. M., Rippeth, T. P., Holligan, P. M., Hydes, D. J., Fisher, N. R., and Simpson, J. H.: Phytoplankton Distribution and Survival in the Thermocline, Limnology and Oceanography, 46, 486–496, 2001.

Siegel, D. A., Doney, S. C., and Yoder, J. A.: The North Atlantic Spring Phytoplankton Bloom and Sverdrup's Critical Depth Hypothesis, Science, 296, 730 –733, doi: 10.1126/science.1069174, 2002.

Siokou-Frangou, I., Christaki, U., Mazzocchi, M. G., Montresor, M., Ribera d'Alcalà, M., Vaque, D., and Zingone, A.: Plankton in the open Mediterranean Sea: a review, Biogeosciences, 7, 1543–1586, doi: 10.5194/bg-7-1543-2010, 2010.

Sosik, H.M., Chisholm, S. C., and Olson, R. J.: Chlorophyll Fluorescence from Single Cells: Interpretation of flow cytometric signals, Limnology and Oceanography, 34-8, 1749-1761, 1989.

Steinberg, D., Carlson, C., Bates, N., Johnson, R., Michaels, A., and Knap, A.: Overview of the US JGOFS Bermuda Atlantic Time-series Study (BATS): a decade-scale look at ocean biology and biogeochemistry, Deep-Sea Research Part II, 48, 1405–1447, 2001.

Strass, V.: On the calibration of large-scale fluorometric chlorophyll measurements from towed undulating vehicles, Deep Sea Research Part A. Oceanographic Research Papers, 37, 525–540, doi: 16/0198-0149(90)90023-O, 1990.

Strickland, J.: Production of organic matter in primary stages of the marine food chain, in: Chemical Oceanography, pp. 477–610, Academic Press, London, J.P. riley and g. skirrow [ed.] edn., 1965.

1 Taupier-Letage, I., Puillat, I., Millot, C., and Raimbault, P.: Biological response to mesoscale
2 eddies in the Algerian Basin, Journal of Geophysical Research: Oceans (1978–2012), 108,
3 2003.

4 Thomalla, S., Fauchereau, N., Swart, S., and Monteiro, P.: Regional scale characteristics of
5 the seasonal cycle of chlorophyll in the Southern Ocean, Biogeosciences, 8, 2849–2866, 2011.

6 Uitz, J., Claustre, H., Morel, A., and Hooker, S.: Vertical distribution of phytoplankton
7 communities in open ocean: An assessment based on surface chlorophyll, Journal of
8 Geophysical Research-Oceans, 111, doi: 10.1029/2005JC003207, 2006.

9 Volpe, G., Nardelli, B. B., Cipollini, P., Santoleri, R., and Robinson, I. S.: Seasonal to
10 interannual phytoplankton response to physical processes in the Mediterranean Sea from
11 satellite observations, Remote Sensing of Environment, 117, 223–235, doi:
12 10.1016/j.rse.2011.09.020, 2012.

13 Xing, X., Morel, A., Claustre, H., Antoine, D., D'Ortenzio, F., Poteau, A., and Mignot, A.:
14 Combined processing and mutual interpretation of radiometry and fluorimetry from
15 autonomous profiling Bio-Argo floats: Chlorophyll a retrieval, journal of geophysical
16 research-oceans, 116, doi: 10.1029/2010JC006899, 2011.

17 Xing, X., Claustre, H., Blain, S., D'Ortenzio, F., Antoine, D., Ras, J., and Guinet, C.:
18 Quenching correction for in vivo chlorophyll fluorescence measured by instrumented elephant
19 seals in the Kerguelen region (Southern Ocean), Limnology and Oceanography - Methods, 10,
20 483–495, 2012.

21 Yoder, J. A., McClain, C. R., Feldman, G. C., and Esaias, W. E.: Annual cycles of
22 phytoplankton chlorophyll concentrations in the global ocean: A satellite view, Global
23 Biogeochemical Cycles, 7, PP. 181–193, doi: 199310.1029/93GB02358, 1993.

24

1   Table 1. Description of sources for fluorescence profiles. In this table, only fluorescence

2   profiles obtained in Mediterranean regions where bathymetry is superior to 100m are counted.

3   Coastal regions have been neglected.

4

	Data source	Number of profiles
Online databases	PANGAEA (http://www.pangaea.de/)	93
	SISMER (http://www.ifremer.fr/sismer/index_FR.htm)	110
	WOD09 (http://www.nodc.noaa.gov/)	94
	OGS database (http://nodc.ogs.trieste.it/cocoon/data/dataset)	689
	SUB-TOTAL	**986**
French cruises	PROSOPE (Claustre et al., 2004)	96
	DYNAPROC (Andersen and Prieur, 2000)	251
	BOUM (Moutin et al., 2012)	573
	ALMOFRONT (Claustre at al., 2000)	1046
	DYFAMED (Marty et al., 2002)	191
	MOOSE-GE (http://hermes.dt.insu.cnrs.fr/moose/)	285
	DEWEX (Durrieu de Madron et al., 2011)	228
	SUB-TOTAL	**2670**
SESAME Program (http://www.sesame-ip.eu/)		1815
MEDAR Program (MEDAR Group., 2002)		228
Bio-Argo (Xing et al.. 2011; http://www.oao.obs-vlfr.fr/web/index.php)		1091
TOTAL		**6790**

5

6

Table 2. ~~Averaged~~Median and interquartile range (IQR) of [Chl-a] at DCM for each geographical ~~point~~location analyzed on Fig. 3 (i.e. yellow diamonds on Fig. 1). ~~Averaged [Chl-a] values~~Median and IQR were computed by ~~averaging~~considering all the DCM depth [Chl-a] estimations extracted from available "DCM" like profiles. IQR is the difference between the third and the first quartile.

	Point: 42°N 5°E (North-West)				Point: 38°N 5°E (South-West)				Point: 36°N 17°E (Ionian)					~~MEAN~~MEDIAN	~~SD~~IQR	
	~~MEAN~~MEDIAN	~~SD~~IQR	N		~~MEAN~~MEDIAN	~~SD~~IQR	N		~~MEAN~~MEDIAN	~~SD~~IQR	N		~~MEAN~~MEDIAN	~~SD~~IQR	
April	1.~~22~~07	0.~~66~~48	26						0.~~73~~70	0.~~24~~26	107		0.~~50~~47	0.~~07~~09	
May	0.~~86~~83	0.~~20~~33	38		0.~~93~~97	0.~~18~~23	9		0.~~73~~71	0.~~24~~25	37		0.~~50~~49	0.~~09~~08	
June	0.~~99~~97	0.~~28~~36	129		1.~~24~~08	~~0.76~~1.26	6		0.~~90~~81	0.~~23~~28	17		0.~~47~~37	0.~~09~~25	
July	0.~~98~~97	0.~~40~~67	67		0.~~86~~84	0.~~17~~20	160		0.~~47~~42	0.~~15~~23	9		0.~~46~~42	0.~~15~~10	
August	0.~~69~~57	0.~~32~~39	45		0.~~84~~73	0.~~40~~36	7		0.~~44~~41	0.~~14~~15	22		0.~~44~~32	0.~~12~~08	
September	0.~~65~~63	0.~~26~~21	41		0.~~99~~62	0.~~98~~16	9		0.~~34~~32	0.~~11~~17	23		0.~~34~~32	0.~~07~~06	
October	~~0.900~~79	0.~~45~~32	33		1.06	0.~~10~~11	6		0.~~48~~43	0.~~24~~13	81		0.~~31~~32	0.~~04~~03	

Tabella formattata

Table 3. ~~Average~~ Median value (bold) and ~~inter~~ first and ninth decile ~~range~~ for parameters: MLD, euphotic depth (Z_e), surface [Chl-a] observed by satellite (Chl_{SAT}) and percentage of chlorophyll content in the upper 20m layer compared to the whole integrated content (F_{surf}/F_T).

	MLD (m)	Z_e (m)	Chl_{SAT} (mg m^{-3})	F_{surf}/F_T (%)
DCM	**~~17~~** **14** 11-27	**72** 57-90	**0.~~15~~13** 0.05-0.27	**~~6~~5%** 2-11
Modified DCM	**~~30~~** **26** 13-52	**52** 37-66	**0.~~39~~32** 0.16-0.63	**~~22~~21%** 13-32
Homogeneous	**~~186~~** **86** 27-596	**~~51~~** **52** 29-71	**0.~~53~~31** 0.13-1.19	**~~32~~21%** 11-43
Complex	**~~39~~** **33** 17-63	**48** 33-62	**0.~~52~~36** 0.18-0.80	**~~30~~28%** 18-47
HSC	**~~57~~** **35** 13-95	**~~36~~** **34** 17-57	**~~1.22~~** **0.77** 0.25-2.76	**~~35~~31%** 20-53

1   Table 4. Regional average values and standard deviations (numbers in brackets) for a set of
2   parameters. Winter MLD was computed with January and February MLDs. The DCM depth
3   and the PAR at DCM has been computed only for profiles belonging to the "DCM" standard
4   shape category. PAR at DCM has been determined for each fully calibrated (i.e. 1998-2014
5   database) [Chl-a] vertical profiles. The vertical profile of the PAR attenuation coefficient was
6   computed from [Chl-a] vertical profile and applied to surface PAR estimates derived from the
7   monthly SeaWiFS PAR climatology. For the nitracline depth, the isoline 1μM was computed
8   on a large set of nitrates profiles derived from MEDAR and SESAME programs (see Lavigne
9   et al., 2013 for details about this database).

10

	Winter MLD (m)	Nitracline depth (m)	DCM depth (m)	PAR at DCM (mol photons m^{-2} day^{-1})
North-West	342 (623)	62 (38)	51.7 (12.5)	1.03 (0.86)
South-West	47 (63)	78 (24)	73 (17)	0.77 (0.77)
Tyrrhenian	45 (38)	97 (23)	73 (13)	0.57 (0.19)
Adriatic	126 (181)	56 (24)	56 (10)	--
Ionian	67 (46)	119 (46)	83 (29)	0.51 (0.64)
Levantine	122 (122)	185 (47)	102 (17)	0.16 (0.16)

11
12
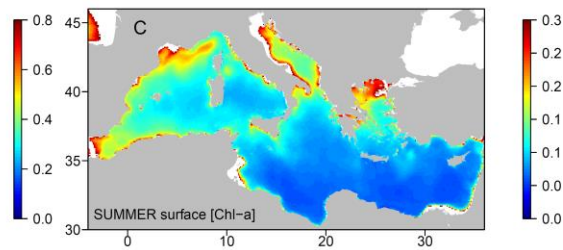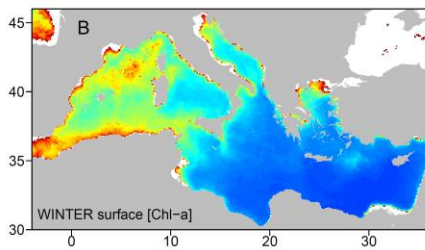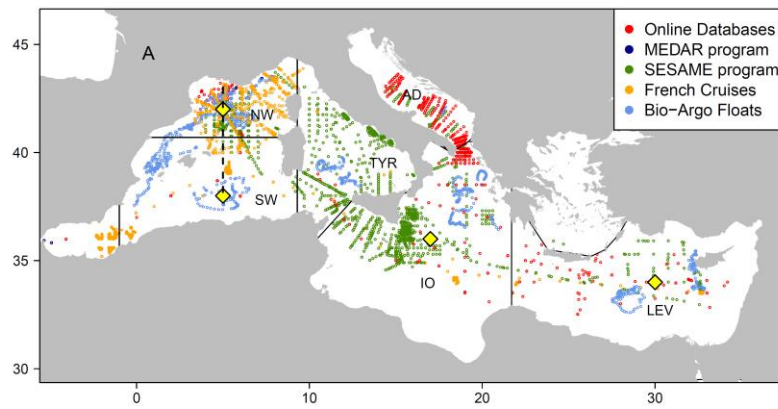
1

2 Figure 1. Panel A: spatial distribution of fluorescence profiles available in the database.

3 Colors indicate the source of data. Black lines delineate large Mediterranean regions: they are

4 referred by NW for "North-West", SW for "South-West", TYR for "Tyrrhenian", AD for

5 "Adriatic", IO for "Ionian" and LEV for "Levantine". Yellow diamonds refer to the center of

6 region for which a climatology of [Chl-a] vertical profile has been computed (see Fig. 3) and

7 the dashed black line shows the center of the North-West transect (see Fig. 4). Panels B and

8 C: SeaWiFS climatology of surface [Chl-a] for winter (panel B) and summer (panel C). Note

9 that color scales are not the same.

10

11

1

A. DCM B. homogeneous C. HSC

D. modified DCM F. complex

2

3
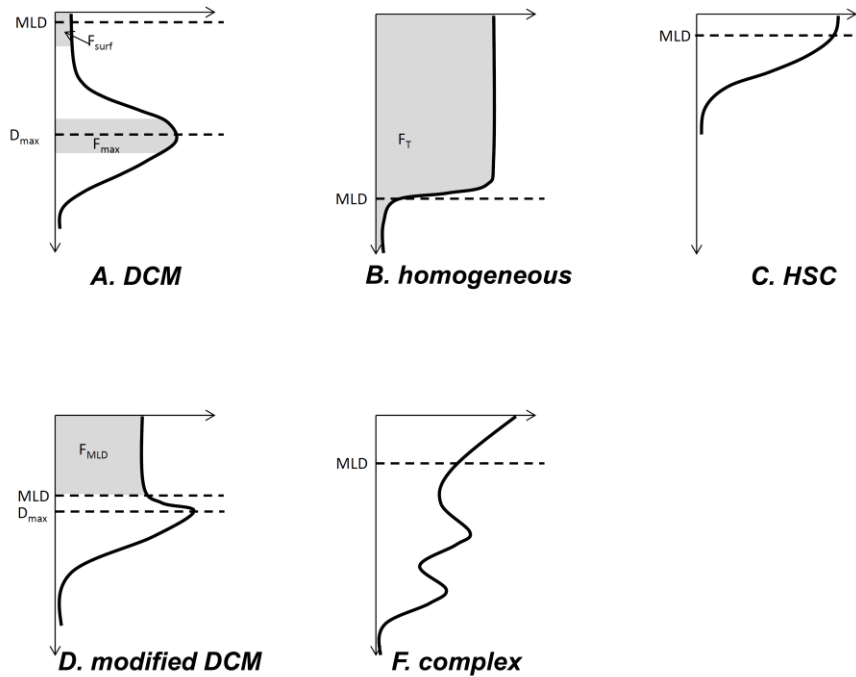
Figure 2. The five standard shapes for [Chl-a] vertical profiles identified in our dataset. See

Sect. 2.3 of the text for more details about these shapes and for a description of the algorithm

used to identify them. Black solid lines represent the normalized [Chl-a] vertical profile.

Metrics used for the determination of the profile standard shape (i.e. MLD, D_{max}, F_{surf}, F_{max},

F_T, see text Sect. 2.3 for definitions) are represented on standard profiles. Although all of

these metrics have been computed on each fluorescence profile, they could not be represented

on a same profile for practical reasons.

11

12

1

2

3
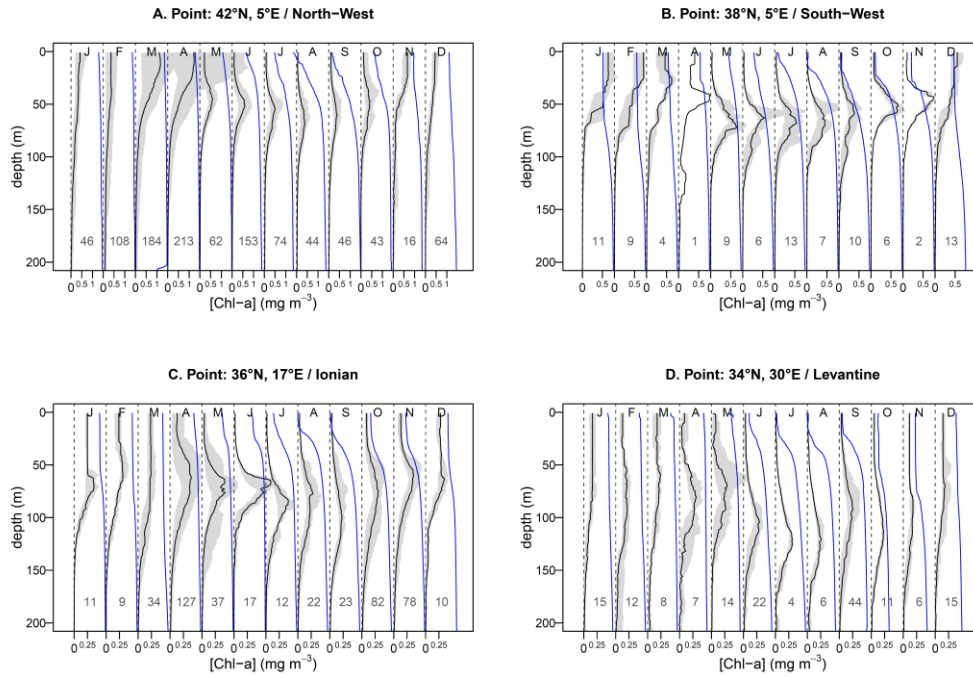
Figure 3. Climatology of [Chl-a] vertical profiles (black lines) for 4 points of the Mediterranean Sea (see yellow diamonds on Fig. 1). All profiles located within a 4°x4° box centered on indicated positions were retained. The median value for each month is the black line. The grey zone indicates the 0.1 quantile – 0.9 quantile range. Numbers below climatological profiles indicate on the number of available data profiles used to compute them. Normalized average water density profiles are superimposed (blue lines).

10

11

from March to May
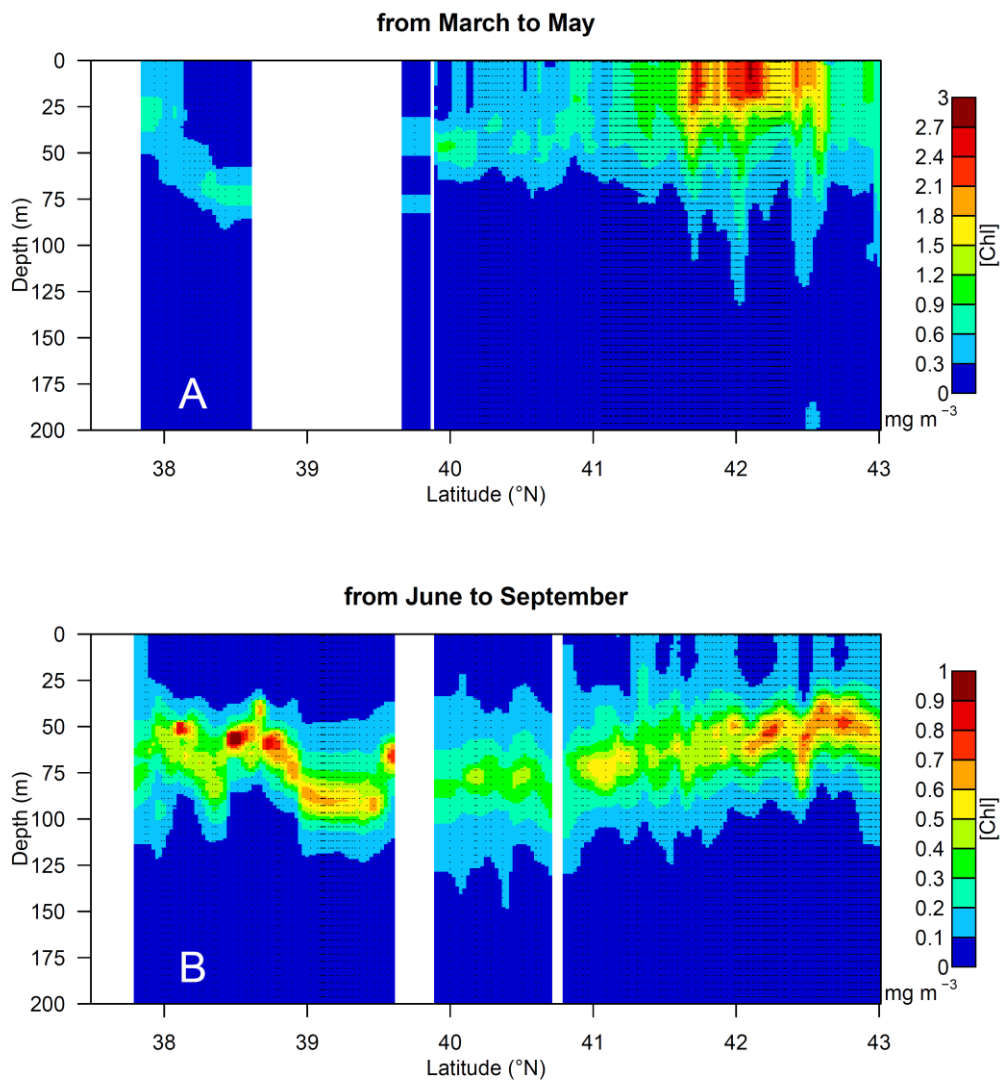
from June to September

Figure 4. North-South climatological transect of [Chl-a] along the 5°W meridian (see the black dotted line on Fig. 1). Panel A represents the averaged situation for the March to May period and panel B for the June to September period. Note that color scales are different between panels A and B. For each available data profile, a vertical dotted line was superimposed to the graphic.
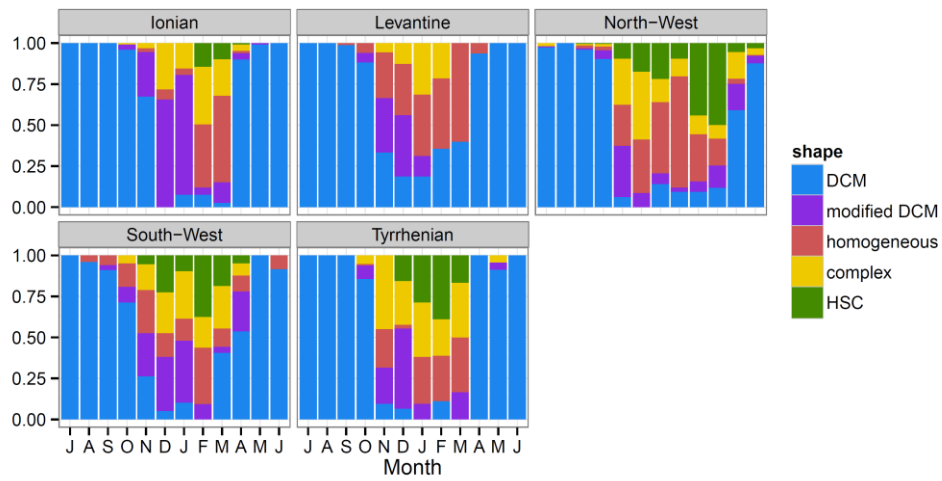
Figure 5. Histograms indicating for each month and each Mediterranean region, the proportion of each type of standard shape observed in the 1994-2014 database (i.e. "DCM", "homogeneous", "HSC", "modified DCM" and "complex" see Fig. 2 and Sect. 2.3). The height of color bars indicates the proportion of profiles which were classed in each category of standard shapes. Note that months range from July to June.
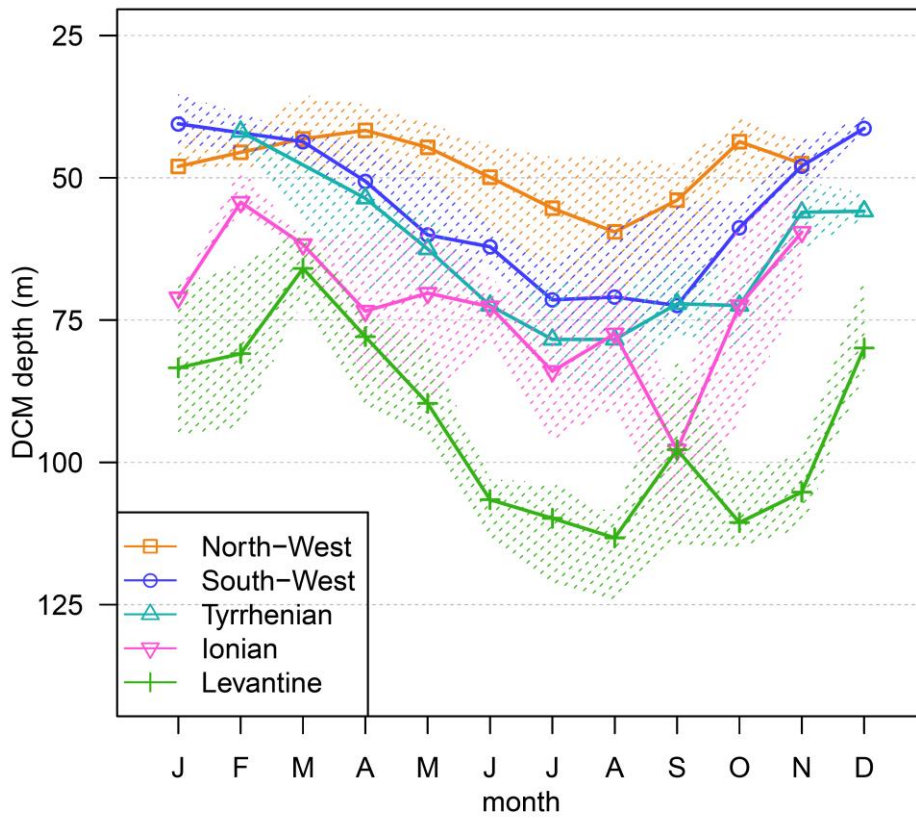
1

2

3
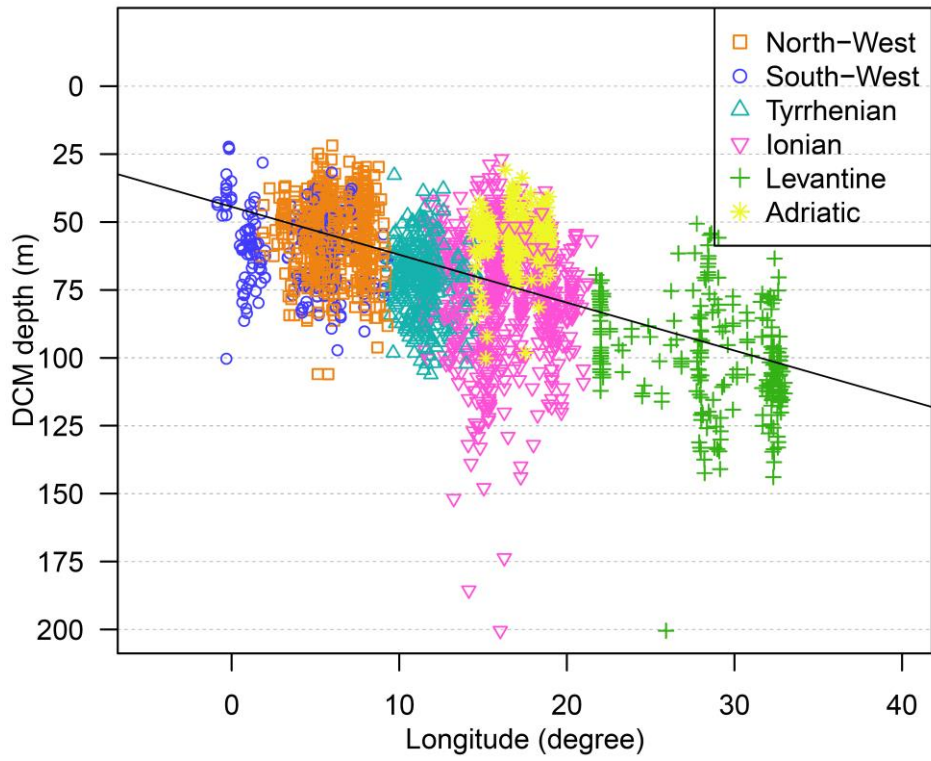
Figure 6. DCM depth as a function of longitude. DCM depths were computed only on "DCM" like profiles (see Sect. 2.3 for an objective definition of "DCM" like profile). Black line represents the linear model between the DCM depth and the longitude. Its slope is 1.6 m per degree of longitude.
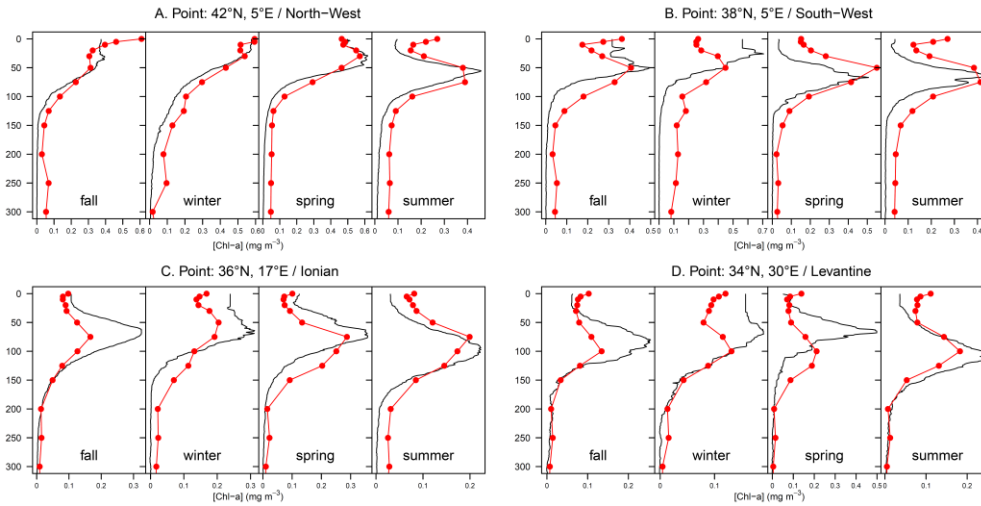
8

9

1

2

3

Figure 7. Seasonal evolution of the DCM depth. DCM depths were computed only on "DCM"

like profiles (see Sect. 2.3 for an objective definition of "DCM" like profile). Symbols refer to

monthly median whereas dotted areas indicate the inter-quartile range.

7

8

1

2

3

4   Figure 8. [Chl-a] profiles obtained from the MEDATLAS climatology for the four locations

5   analyzed on Fig. 3 (red lines and red points). MEDATLAS climatology was downloaded from

6   http://modb.oce.ulg.ac.be/backup/medar/medar_med.html. For comparison, corresponding

7   seasonally averaged profiles were computed from the 1998-2014 [Chl-a] fluorescence

8   database (black lines). Seasons are calendar-based seasons.

9

10

1

2
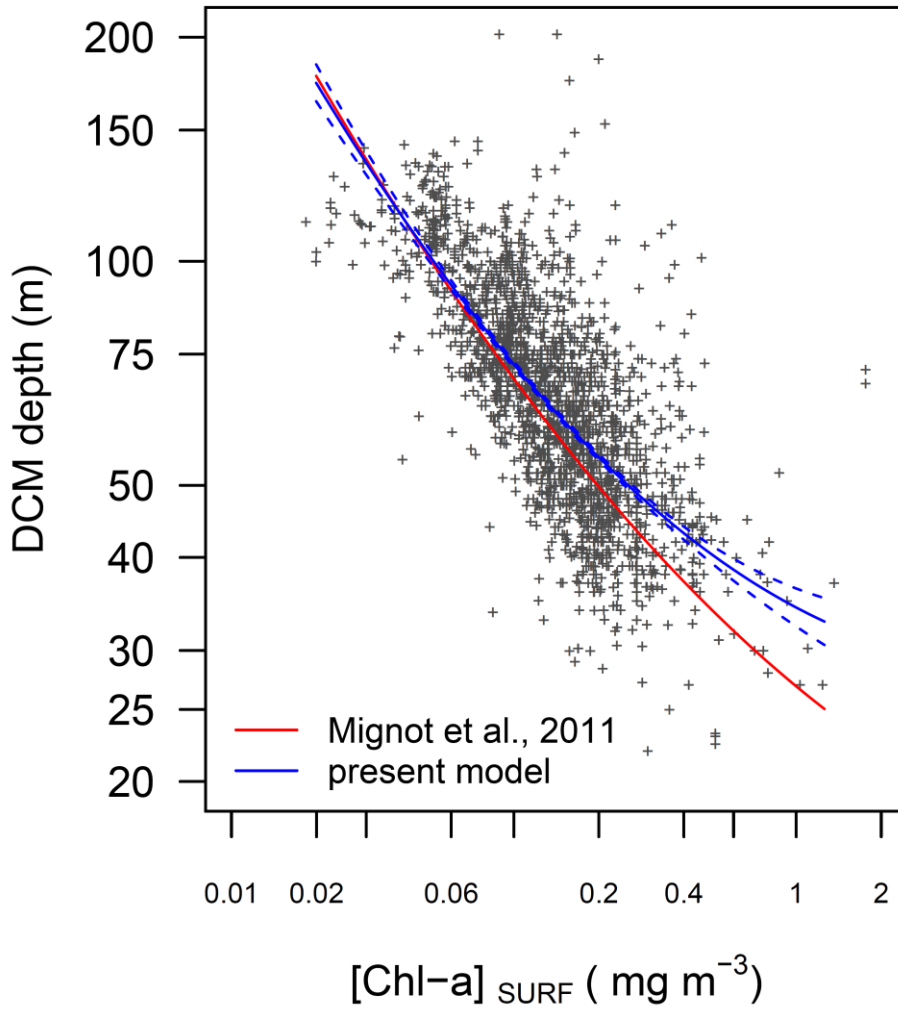
Figure 9. Scatter plots of the DCM depth as a function of surface [Chl-a]. Only "DCM" like profiles were used for this analysis. Surface [Chl-a] were obtained from satellite ocean color data. The blue solid line refers to a second order polynomial model determined from present data $(R^2 = 0.52)$ with its confidence intervals (blue dotted lines) and the red line represents model computed by Mignot et al. (2011) from a global ocean dataset.

8
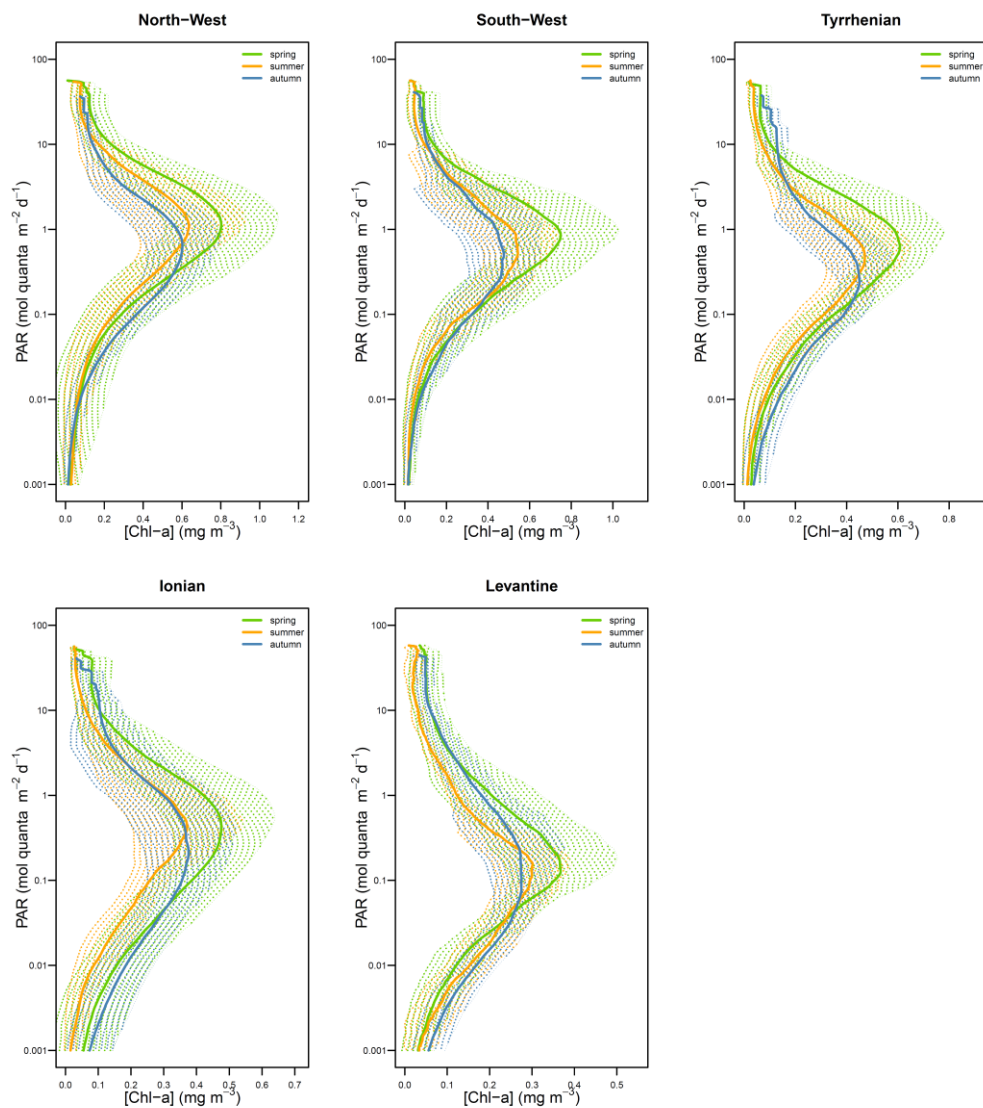
1

2 Figure 10. Averaged vertical distribution of [Chl-a] as a function of PAR with standard

3 deviation (dotted area). Spring refers to the April-June period, summer to July and August and

4 autumn to the September-November period.